https://doi.org/10.1093/plcell/koac164 THE PLANT CELL 2022: 34: 3425–3442

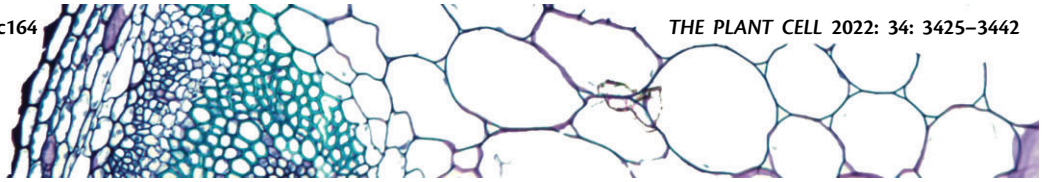

Research Article

Phosphorylation of OsTGA5 by casein kinase II compromises its suppression of defense-related gene transcription in rice

Yuqing Niu [1], Xiaoguang Huang [1], Zexue He [2], Qingqing Zhang [1], Han Meng [1], Hua Shi [1], Baomin Feng [1], Yuanchang Zhou [1,*], Jianfu Zhang [3], Guodong Lu [4], Zonghua Wang [5], Wenli Zhang [2], Dingzhong Tang [1] and Mo Wang [1,*]

1 Key Laboratory of Ministry of Education for Genetics, Breeding and Multiple Utilization of Crops, Fujian University Key Laboratory for Plant–Microbe Interaction, Ministerial and Provincial Joint Innovation Centre for Safety Production of Cross-Strait Crops, Fujian Agriculture and Forestry University, Fuzhou 350002, China
2 State Key Laboratory for Crop Genetics and Germplasm Enhancement, JiangSu Collaborative Innovation Center for Modern Crop Production, Nanjing Agricultural University, Nanjing 210095, China
3 Rice Research Institute, Fujian Academy of Agricultural Sciences, Fuzhou 350019, China
4 Key Laboratory of Biopesticides and Chemical Biology, Ministry of Education, Fujian Agriculture and Forestry University, Fuzhou 350002, China
5 Institute of Oceanography, Minjiang University, Fuzhou 350108, China

*Author for correspondence: zwy_2002@163.com (Y.Z.), wangmo108@163.com (M.W.)
M.W., W.Z., B.F., and Y.Z. conceived and designed the project. Y.N., X.H., Z.H., Q.Z., and H.S. performed the experiments. M.W. and J.Z. created the rice materials. M.W., Y.N., and W.Z. wrote the manuscript. H.S., G.L., Z.W., Y.Z., and D.T. revised and edited the manuscript.
The author responsible for distribution of materials integral to the findings presented in this article in accordance with the policy described in the Instructions for Authors (https://academic.oup.com/plcell) is: Mo Wang (wangmo108@163.com).

Abstract

Plants manage the high cost of immunity activation by suppressing the expression of defense genes during normal growth and rapidly switching them on upon pathogen invasion. TGAs are key transcription factors controlling the expression of defense genes. However, how TGAs function, especially in monocot plants like rice with continuously high levels of endogenous salicylic acid (SA) remains elusive. In this study, we characterized the role of OsTGA5 as a negative regulator of rice resistance against blast fungus by transcriptionally repressing the expression of various defense-related genes. Moreover, OsTGA5 repressed PTI responses and the accumulation of endogenous SA. Importantly, we showed that the nucleus-localized casein kinase II (CK2) complex interacts with and phosphorylates OsTGA5 on Ser-32, which reduces the affinity of OsTGA5 for the *JIOsPR10* promoter, thereby alleviating the repression of *JIOsPR10* transcription and increasing rice resistance. Furthermore, the in vivo phosphorylation of OsTGA5 Ser-32 was enhanced by blast fungus infection. The CK2 α subunit, depending on its kinase activity, positively regulated rice defense against blast fungus. Taken together, our results provide a mechanism for the role of OsTGA5 in negatively regulating the transcription of defense-related genes in rice and the repressive switch imposed by nuclear CK2-mediated phosphorylation during blast fungus invasion.

Received July 12, 2021. Accepted April 25, 2022. Advance access publication June 1, 2022

In A NUTSHELL

Background: Plants balance the high cost of immunity by suppressing the expression of defense genes during normal growth, while rapidly switching them on when perceiving pathogens. The regulation of the transcription factors (TFs) controlling the transcription of defense genes plays an essential role in this switch. TGA-type TFs are key regulators of plant innate immunity. In Arabidopsis, pathogen attacks dramatically increase endogenous salicylic acid (SA) levels, which promote the nuclear enrichment of the NONEXPRESSER OF PR GENES 1 monomer, which helps dissociate the TGA2 oligomer into a dimer to induce the transcription of *Pathogenesis-related* (*PR*) genes. Although this signaling pathway plays a critical role in boosting immunity in Arabidopsis, how TGA activity is regulated in monocots is largely unknown.

Question: How do plant species such as rice, with constant high levels of SA even during pathogen infection, regulate TGA activity? This is a critical question, because rice TGA2.1 has been found to suppress the transcription of defense genes during normal growth and inhibit immunity against the bacterial pathogen.

Findings: OsTGA5, the closest rice homolog to Arabidopsis TGA2, negatively regulates rice resistance against blast fungus by blocking the transcription of various defense-related genes. We discovered that the nucleus-localized casein kinase II (CK2) complex interacts with and phosphorylates OsTGA5 at Ser-32, which is enhanced upon blast fungus infection. This phosphorylation decreases the binding of OsTGA5 to the promoter of the rice *PR* gene, thereby alleviating the transcriptional repression by OsTGA5 and promoting resistance against blast fungus. Thus, this CK2-based phosphorylation mechanism is an important molecular switch in rice involved in elevating the expression of defense genes normally suppressed by TGA upon pathogen invasion.

Next steps: We wish to explore the interplay, including functional redundancy or differentiation, and the formation of hetero- or homo-oligomers, between rice TGA members in controlling the transcription of defense genes. Moreover, determining the influence of CK2-mediated phosphorylation on rice TGAs interplay will help scientists to better understand how TGAs are regulated in rice.

Introduction

Plants deploy sophisticated defense systems to protect themselves from invasion by pathogenic microorganisms (Chisholm et al., 2006). In the early stage of infection, pathogen-associated molecular patterns (PAMPs) are perceived by pattern recognition receptors (PRRs) located at the cell membrane, which rapidly activate PAMP-triggered immunity (PTI) responses, including reactive oxygen species (ROS) bursts, mitogen-activated protein kinase (MAPK) cascade activation, calcium influx, and callose deposition (Dodds and Rathjen, 2010; Macho and Zipfel, 2014). To overcome this horizontal plant resistance, pathogens secrete effectors to disrupt PTI signaling pathways. Plant resistance I proteins, characterized by nucleotide-binding site (NBS) and leucine-rich repeat (LRR) domains, can recognize a subset of these effectors and induce a strong isolate-specific resistance, called effector-triggered immunity (ETI), which is often coupled with a hypersensitive response (HR), a form of programmed cell death (Alhoraibi et al., 2019). As a common feature of both PTI and ETI, transcriptional reprogramming, governed by transcription factors (TFs) and coregulatory proteins, is essential for increasing plant resistance by upregulating defense-related gene expression (Tsuda and Katagiri, 2010). Accumulating evidence indicates that certain plant TF families, such as ETHYLENE-RESPONSIVE FACTOR, basic leucine zipper (bZIP), basic helix-loop-helix, WRKY, NAM, ATAF, CUC (NAC), and MYB, control the activation of innate immunity (Tsuda and Somssich, 2015).

The TGA family of TFs is conserved in land plants and belongs to the bZIP super family of TFs, which contains 78 and 89 members in Arabidopsis (*Arabidopsis thaliana*) and rice (*Oryza sativa*), respectively (E et al., 2014; Dröge-Laser et al., 2018). Tobacco (*Nicotiana tabacum*) TGA1a was the first plant TF to be cloned, based on its ability to bind to the TGACGT sequence in the *activation sequence-1* (*as-1*) element of the cauliflower mosaic virus 35S promoter (Katagiri et al., 1989). Since the discovery of this family, many studies have shown that TGA TFs function in plant defense responses against biotic and abiotic stresses (Gatz, 2013). The TGAs within the D subgroup of the Arabidopsis bZIP TF family are mainly involved in regulating pathogenesis-related (*PR*) gene expression through the salicylic acid (SA) signaling pathway, and they can be further classified into three clades: clade I (TGA1 and TGA4), clade II (TGA2, TGA5, and TGA6), and clade III (TGA3 and TGA7) (Jakoby et al., 2002). Members of clade II interact with the positive regulator NONEXPRESSER OF PR GENES 1 (NPR1) and are essential for SA-induced *PR* gene expression and systemic acquired resistance (SAR) (Després et al., 2000; Fan and Dong, 2002). Both SA-induced *PR1* expression and SAR activation are abolished in the *tga2 tga5 tga6* triple mutant (Zhang et al., 2003). However, clade II member TGA2 was shown to function as a negative regulator of *PR* transcription (Kesarwani et al., 2007). In rice, four TGA TFs, OsTGA2, rTGA2.1, OsTGA3 (also named rTGA2.2), and OsTGA5 (rTGA2.3), are grouped in the same clade as Arabidopsis

TGA2/5/6 and interact with Arabidopsis NPR1 or its rice homologs NPR1 HOMOLOGs (NHs) (Moon et al., 2018). Of these, two TGAs have been functionally characterized in immunity; rTGA2.1 plays a negative role in rice basal defense against the bacterial pathogen *Xanthomonas oryzae* pv. *oryzae* (*Xoo*) (Fitzgerald et al., 2005), while OsTGA2 functions in the positive control of defense-related gene expression and resistance to *Xoo* (Moon et al., 2018). Therefore, TGA factors, despite being highly similar in sequence, exert distinct activities in regulating immune gene expression.

Casein kinase II (CK2) is a conserved serine/threonine kinase tetramer in eukaryotes that is composed of two catalytic α and two regulatory β subunits. CK2 in plants plays essential roles in regulating various physiological processes, such as light signaling, circadian rhythms, and phytohormone responses (Mulekar and Huq, 2014). There are four CK2α subunits in Arabidopsis, of which three localize to the nucleus and exhibit redundant functions in regulating circadian rhythms (Lu et al., 2011); the other CK2α functions in chloroplasts (Salinas et al., 2006). In rice, OsCK2α3, residing in the endoplasmic reticulum (ER) compartment, phosphorylates

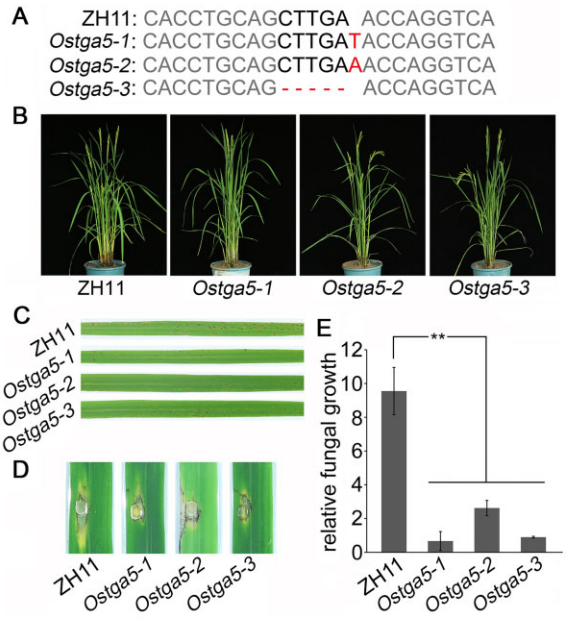

Figure 1 Ostga5 mutants display increased resistance to *M. oryzae*. A, Mutation sites of *OsTGA5* knockout mutants generated by CRISPR/Cas9 genome editing in ZH11. B, The *Ostga5* mutants exhibit no obvious growth or developmental defect, compared with the wild-type. The plants were grown in the field and imaged at the heading stage. C, Three-week-old seedlings of ZH11 and *Ostga5* mutants inoculated with *M. oryzae* conidia (isolate Guy11) by spraying. The leaves of *Ostga5* mutants have fewer disease lesions than those of ZH11. Images were taken 5 dpi. D, Five-week-old plants of ZH11 and *Ostga5* mutants were subjected to punch inoculation with Guy11 conidia. The diseased leaves were photographed at 9 dpi. E, Fungal biomass of punch-inoculation leaves was measured to quantify relative *M. oryzae* growth (fungal biomass) in ZH11 and *Ostga5* mutants. Data are means ± SE from three biological replicates. Significant differences were determined by one-way ANOVA (**$P < 0.01$).

PHOSPHATE TRANSPORTER 8 and prevents its exit from the ER under phosphate-sufficient conditions (Chen et al., 2015); another rice *Ck2α* gene, named as *Heading date 6* (*Hd6*), was cloned within the quantitative trait locus controlling flowering time, whose encoded protein localizes to the nucleus and delays the heading date under natural and long-day conditions (Takahashi et al., 2001; Kwon et al., 2015). Interestingly, the *Hd6* allele present in the *japonica* variety Nipponbare carries a premature stop codon, leading to a truncated and nonfunctional protein (Takahashi et al., 2001). To date, biological functions of the unique nucleus-localized CK2α in *japonica* rice varieties are ambiguous. Moreover, the potential roles and mechanisms of plant CK2αs in regulating plant defense against pathogens are still unclear.

Rice blast disease, caused by the ascomycete pathogen *Magnaporthe oryzae*, is among the most devastating diseases threatening rice yield and leads to enormous yearly production losses worldwide. Characterizing the genes negatively regulating rice immunity, especially those with moderate roles in growth and development, is a promising approach for controlling rice blast disease through current gene-editing technology (Chen et al., 2019). In this study, we describe the negative roles of OsTGA5 in regulating immune responses against *M. oryzae* and reveal its function as a transcriptional repressor of various putative defense-related genes in rice. Interestingly, the nucleus-localized CK2 complex interacts with and phosphorylates OsTGA5, which reduces the affinity of OsTGA5 to the binding motif within the promoter of *Jasmonate-inducible PR10* (*JIOsPR10*) and alleviates its transcriptional suppression to mount resistance.

Results

Loss of OsTGA5 function confers enhanced rice resistance to blast fungus

To reach a better understanding of TGA-based regulation of rice immunity and identify the TGA member repressing rice defense against blast fungus, we functionally characterized the rice homolog of Arabidopsis TGA2. Through protein sequence alignment, we determined that among the rice TGA TFs within clade II, OsTGA5 is the most closely related to Arabidopsis TGA2 (Supplemental Figure S1). To explore the involvement of OsTGA5 in rice immunity, we used clustered regularly interspaced short palindromic repeats (CRISPR)/CRISPR-associated nuclease 9 (Cas9)-mediated genome editing to generate knockout mutants of *OsTGA5* (*Ostga5*) in the rice *japonica* cultivar Zhonghua11 (ZH11). We obtained three homozygous *Ostga5* mutants from independent primary transgenic plants. As shown in Figure 1A, the *Ostga5-1* and *Ostga5-2* mutants harbored a 1-bp insertion between nucleotides 65 and 66 of the OsTGA5 coding region, while *Ostga5-3* carried a 5-bp deletion between nucleotides 61 and 65. All three alleles resulted in a frameshift in the *OsTGA5* coding region. When grown in a plot, these three *Ostga5* mutants displayed no obvious defects in growth or development compared with ZH11 (Figure 1B and Supplemental

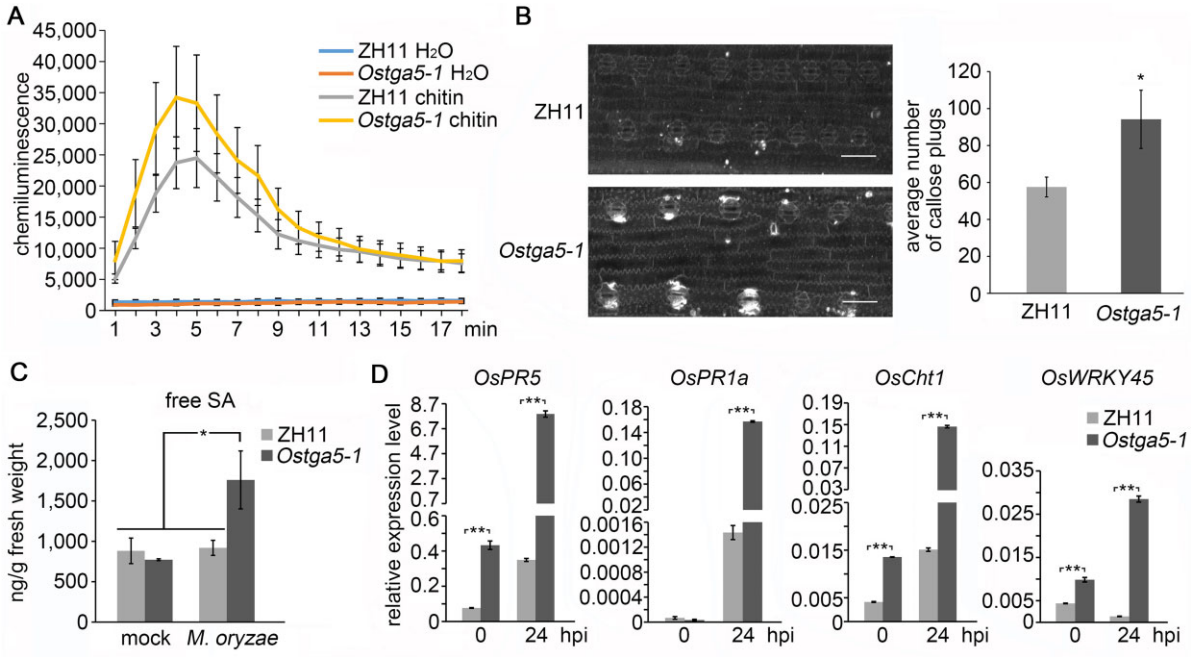

Figure 2 Loss of OsTGA5 function enhances immune responses. A, Time course of ROS burst generated from ZH11 and *Ostga5-1* leaf discs treated with 400 nM chitin. Data are means ± SE (n = 16). The data are from one representative out of three independent experiments. B, Chitin-induced callose deposition on ZH11 and *Ostga5-1* leaves. The rice leaves were treated with 400 nM chitin, and callose deposition was imaged with a microscope under UV light (left), scale bars = 50 μm. The amount of callose deposition was quantified with ImageJ (right). Data are means ± SE (n = 18, randomly chosen leaf regions of interest). Significant differences were determined by one-way ANOVA (*$P < 0.05$). This assay was performed in three independent replicates with similar results. C, Free SA contents in ZH11 and *Ostga5-1* seedlings with or without inoculation with Guy11, as measured by ultra-performance LC–MS/MS. Data are means ± SE from three biological replicates. Significant differences were determined by one-way ANOVA (*$P < 0.05$). D, Relative transcript levels of defense-related genes in the SA signaling pathway in ZH11 and *Ostga5-1* before and after spraying inoculation with Guy11 conidia, as analyzed by RT-qPCR. Rice *UBQ* was used as the internal control. Data are means ± SE (n = 3). Significant differences were determined by one-way ANOVA (**$P < 0.01$). The data are from one of three independent representative experiments.

Figure S2). When challenged with conidial spores for *M. oryzae* isolate Guy11, which is virulent toward ZH11, we observed far fewer disease lesions on the leaves of *Ostga5* mutants compared with those on the wild-type (Figure 1C). To quantify the resistance of *Ostga5* mutants to blast fungus, we carried out punch inoculation assays with the leaves of *Ostga5-1*, *Ostga5-2*, *Ostga5-3*, and ZH11, and investigated the relative fungal biomass within the infected regions. The *Ostga5* mutants supported significantly less blast fungus growth than ZH11 ($P < 0.01$; Figure 1, D and E). We also performed a rice leaf sheath inoculation assay to monitor *M. oryzae* invasion in *Ostga5-1* and ZH11. The invasive hyphae (IH) of Guy11 extended to the neighboring cells of the first infected cell in ZH11 at 48-h postinoculation (hpi) and further extended to the adjacent cells at 72 hpi (Supplemental Figure S3). However, the IH in *Ostga5-1* leaf sheath cells was notably thinner than those in ZH11, and at 72 hpi, the extension of IH in *Ostga5-1* was markedly slower than that in ZH11 (Supplemental Figure S3). In addition, we challenged *Ostga5-1* with another blast fungal isolate, ZHONG1, which is virulent to ZH11 as well, and determined that *Ostga5-1* also displays increased resistance to ZHONG1 compared with the wild-type (Supplemental Figure S4). Taken together, our data indicate that OsTGA5 is a negative regulator of rice resistance against blast fungus.

The immune responses of *Ostga5-1* mutant are enhanced

To better understand the enhanced resistance against *M. oryzae* in the absence of OsTGA5, we investigated PTI responses of *Ostga5-1* and ZH11 induced by chitin. First, we measured the ROS burst from *Ostga5-1* and ZH11 leaves upon chitin treatment, which revealed higher ROS burst levels in *Ostga5-1* than in ZH11 at the tested time points (Figure 2A). Moreover, we observed a nearly 40% increase in callose deposition in *Ostga5-1* leaves compared with ZH11, as detected by the autofluorescence emitted by callose under ultraviolet (UV) light (Figure 2B). In addition, we determined the contents of the defense-related phytohormones salicylic acid (SA) and jasmonic acid (JA) in *Ostga5-1* and ZH11 plants with and without *M. oryzae* infection. The free SA levels were similar in *Ostga5-1* and ZH11 under mock treatment, whereas *M. oryzae* inoculation stimulated the accumulation of SA in the *Ostga5-1* mutant about two-fold relative to mock-treated plants, but not in ZH11 (Figure 2C). In contrast, the JA levels in *Ostga5-1* and ZH11 plants with or without *M. oryzae* infection were not notably different (Supplemental Figure S5). To verify the higher SA levels in the *Ostga5* mutant following *M. oryzae* invasion, we investigated the transcript levels of the genes *OsPR5*, *OsPR1a*, *Chitinase 1* (*OsCht1*), and *OsWRKY45* in the SA-mediated

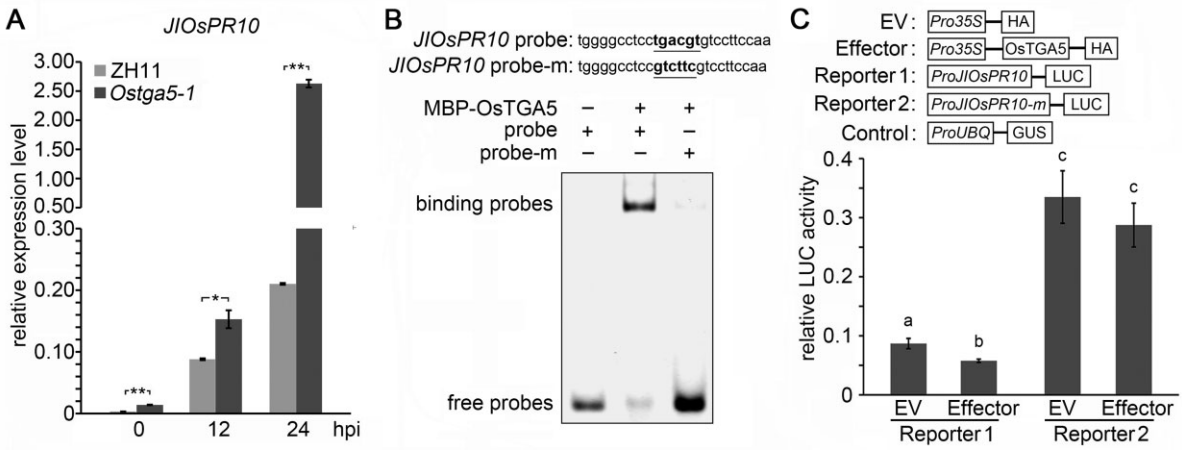

Figure 3 OsTGA5 suppresses *JIOsPR10* transcription by binding to the TGACGT motif in its promoter. A, Relative transcript levels of *JIOsPR10* in ZH11 and the *Ostga5-1* mutant before and after spray-inoculation with Guy11 conidia, by RT-qPCR. *UBQ* served as the internal control. Data are means ± SE ($n = 3$). Significant differences were determined by one-way ANOVA (**$P < 0.01$; *$P < 0.05$). This assay was performed in three independent replicates with similar results. B, OsTGA5 binds to the DNA fragment of the *JIOsPR10* promoter containing the TGACGT motif, as determined by EMSA. Sequences of the probe and mutated probe are indicated at the top. Recombinant OsTGA5 protein (5 μg) was incubated with intact (lane 2) or mutated (lane 3) probe. C, OsTGA5 suppresses transcription from the *JIOsPR10* promoter in ZH11 protoplasts when the TGACGT motif is present. Top, schematic diagrams of the constructs used in this assay. Bottom, relative LUC activity (normalized luminescence) of each indicated construct combination was calculated as luminescence/GUS activity. Data are means ± SE ($n = 10$). Different lowercase letters indicate significant differences ($P < 0.01$, one-way ANOVA). This result is from one representative out of three independent experiments.

defense pathway (Agrawal et al., 2000; Rakwal et al., 2001; Shimono et al., 2007; Hao et al., 2012) before and after *M. oryzae* infection. We established that the transcript levels of all these genes are significantly higher in *Ostga5-1* plants after inoculation compared with those in ZH11 ($P < 0.01$; Figure 2D). Therefore, we conclude that loss of OsTGA5 function enhances the chitin-induced immune responses including ROS burst and callose deposition, and elevates endogenous SA levels upon blast fungus invasion.

Several lines of evidence support the idea that SA biosynthesis in rice mainly relies on the phenylalanine ammonia-lyase (PAL) pathway (Duan et al., 2014; Lefevere et al., 2020). Thus, to determine whether the increased resistance in the absence of OsTGA5 is dependent on the higher accumulation of SA, we treated ZH11 and *Ostga5-1* with 2-aminoindane-2-phosphonic acid (AIP), an effective competitive inhibitor of PAL (Wang et al., 2018), for 24 h, and then inoculated the plants with Guy11 conidial spores by spraying. Compared with the mock treatment, AIP diminished the resistance of both ZH11 and *Ostga5-1* plants (Supplemental Figure S6). Notably, *Ostga5-1* plants still developed significantly fewer disease lesions than the wild-type after AIP treatment, suggesting that higher SA accumulation partially contributes to the enhanced resistance of *Ostga5-1* against *M. oryzae*.

OsTGA5 binds to the TGACGT motif in the *JIOsPR10* promoter and represses its transcription

To further characterize the negative regulation of rice immunity by OsTGA5, we analyzed the transcript levels of three known defense-related genes in ZH11 and the *Ostga5-1* mutant before and after inoculation. *JIOsPR10* was originally identified as a defense gene specifically induced by JA/SA and blast fungus infection (Jwa et al., 2001), and overexpression of *JIOsPR10* can enhance rice resistance to blast fungus (Wu et al., 2016). *OsPR10b* is a *PR* gene that is upregulated upon *M. oryzae* infection (Mcgee et al., 2001). *OsNAC4* encodes a plant-specific TF involved in plant hypersensitive cell death (Kaneda et al., 2009). As indicated by reverse transcription-quantitative PCR (RT-qPCR) assays, all three genes exhibited significantly higher resting and *M. oryzae*-induced transcript levels in *Ostga5-1* than in ZH11 (Figure 3A and Supplemental Figure S7), indicating that OsTGA5 represses the transcription of multiple defense-related genes in rice.

Rice TGA subclade II members are known to selectively bind to the DNA sequence TGACGT (Moon et al., 2018). We identified one copy of this sequence in the *JIOsPR10* promoter region (274–279 bp upstream from the transcription start site, TSS). To investigate whether OsTGA5 can physically bind to the *JIOsPR10* promoter, we synthesized a 50-bp fragment of the *JIOsPR10* promoter containing the TGACGT motif (*JIOsPR10* probe) to perform an electrophoretic mobility shift assay (EMSA). We also produced a variant fragment carrying the sequence GTCTTC instead of TGACGT (*JIOsPR10* probe-m) to determine whether TGACGT is required for binding. We observed that recombinant purified maltose-binding protein (MBP)-OsTGA5 protein can bind to the intact *JIOsPR10* probe, causing a shift in the mobility of the oligonucleotide probe, but not to the mutated probe (Figure 3B). This result demonstrates that OsTGA5 can bind to the *JIOsPR10* promoter by targeting the TGACGT motif.

To assess whether OsTGA5 suppresses *JIOsPR10* transcription in vivo, we designed a construct expressing the firefly

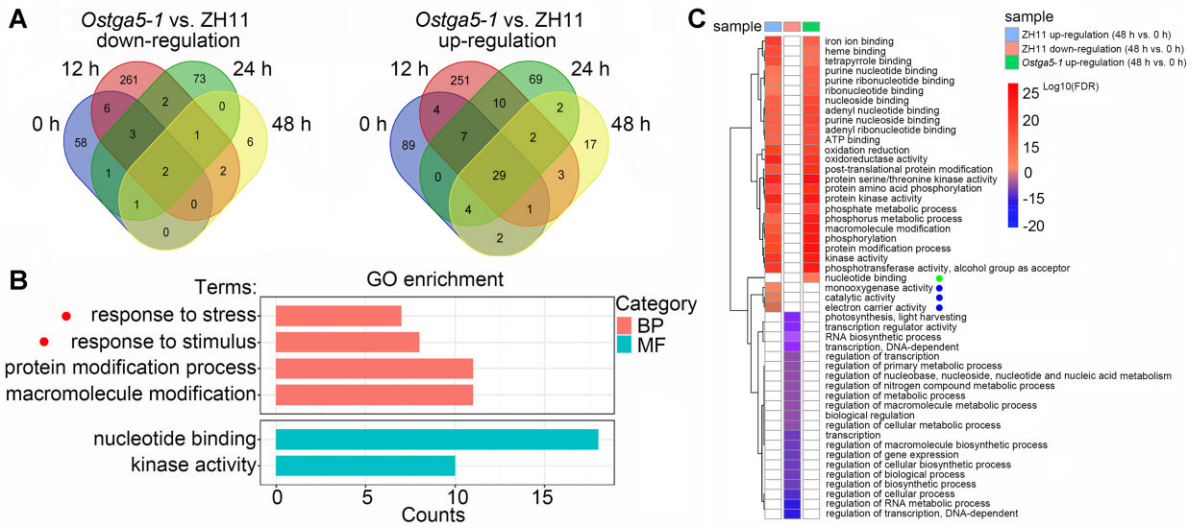

Figure 4 Identification of DEGs in *Ostga5-1* and ZH11 by RNA-seq. A, Venn diagrams showing the number of downregulated (left) or upregulated (right) genes in *Ostga5-1* relative to ZH11 before and at different time points after *M. oryzae* inoculation. B, GO term enrichment analyses of all upregulated genes in *Ostga5-1* containing the TGACGT motif in their promoters. Red circles indicate the terms where putative defense-related genes are enriched. BP, biological process; MF, molecular function. C, GO enrichment analyses using the DEGs identified in *Ostga5-1* and ZH11 at 48 hpi relative to 0 hpi. The term of nucleotide binding (indicated by green circle) and the terms of monooxygenase activity, catalytic activity and electron carrier activity (indicated by blue circles) are specifically enriched in Ostga5-1 and ZH11, respectively.

luciferase (*LUC*) reporter gene under the control of the *JIOsPR10* promoter (a 2,022-bp fragment upstream of the TSS), which we named Reporter 1. We also generated a mutated version of Reporter 1 harboring the same mutation in the TGACGT motif as in the *JIOsPR10* probe-m used for EMSA (named Reporter 2). As a control, we used the *ß-GLUCURONIDASE* (*GUS*) reporter gene under the control of an Arabidopsis *UBIQUITIN* (*UBQ*) promoter. We then co-transfected the Reporter 1 construct and a plasmid expressing *OsTGA5-HA* into rice protoplasts: relative LUC activity was significantly lower than when Reporter 1 was co-transfected with the empty HA vector control (EV) (Figure 3C). Notably, relative LUC activity from Reporter 2 (with the mutated *JIOsPR10* promoter) co-transfected with EV increased to over three-fold over that from Reporter 1 with EV. We also noticed that the repressing effect imposed by OsTGA5 on relative LUC activity from Reporter 2 was abolished (Figure 3C). Taken together, our data indicate that OsTGA5 suppresses *JIOsPR10* transcription by binding to the TGACGT motif within its promoter.

OsTGA5 suppresses the transcription of multiple genes involved in various defense pathways

To identify the complement of defense-related genes under the control of OsTGA5 in the rice genome, we performed transcriptome deep sequencing (RNA-seq) of ZH11 and *Ostga5-1* leaves harvested before (0 h) and 12, 24, and 48 h after Guy11 inoculation. We conducted a pairwise comparison to identify differentially expressed genes (DEGs; upregulated or downregulated genes with fold-change >2) between *Ostga5-1* and ZH11, which revealed more upregulated genes in *Ostga5-1* relative to ZH11 at the different time points compared with the number of downregulated genes (Supplemental Table S1). Two and 29 genes were consistently downregulated and upregulated, respectively, in *Ostga5-1* compared with ZH11 at all time points, suggesting a repressive role for OsTGA5 in transcription during the activation of rice innate immunity (Figure 4A). Furthermore, we selected all DEGs containing an OsTGA5-binding motif in their promoters (defined as 2,000 bp upstream from the TSSs, Supplemental Table S1), and used them to conduct a Gene Ontology (GO) enrichment analysis. The upregulated genes in *Ostga5-1*, but not the downregulated genes, were enriched for terms related to various biological processes and molecular functions (Figure 4B). In particular, the two biological processes, response to stress and stimulus (highlighted by red dots in Figure 4B), were enriched with eight genes, including one *PR* gene, three genes encoding NBS-LRR proteins and two genes encoding peroxidases (Supplemental Table S2), suggesting that OsTGA5 directly suppresses the transcription of these genes involved in immunity.

Considering the drastic changes in the local growth environment, such as continuous darkness and high humidity during the first 24 hpi, we focused on with the DEGs in *Ostga5-1* and ZH11 at 48 hpi to exclude effects arising from the inoculation conditions and to identify OsTGA5-regulated genes specifically involved in defense pathways. Accordingly, we plotted the transcript profiles of the DEGs in *Ostga5-1* and ZH11 at 48 hpi relative to those at 0 hpi (48 versus 0 h; Figure 4C). Interestingly, in contrast to DEGs in ZH11 48 versus 0 h, none of the downregulated genes in

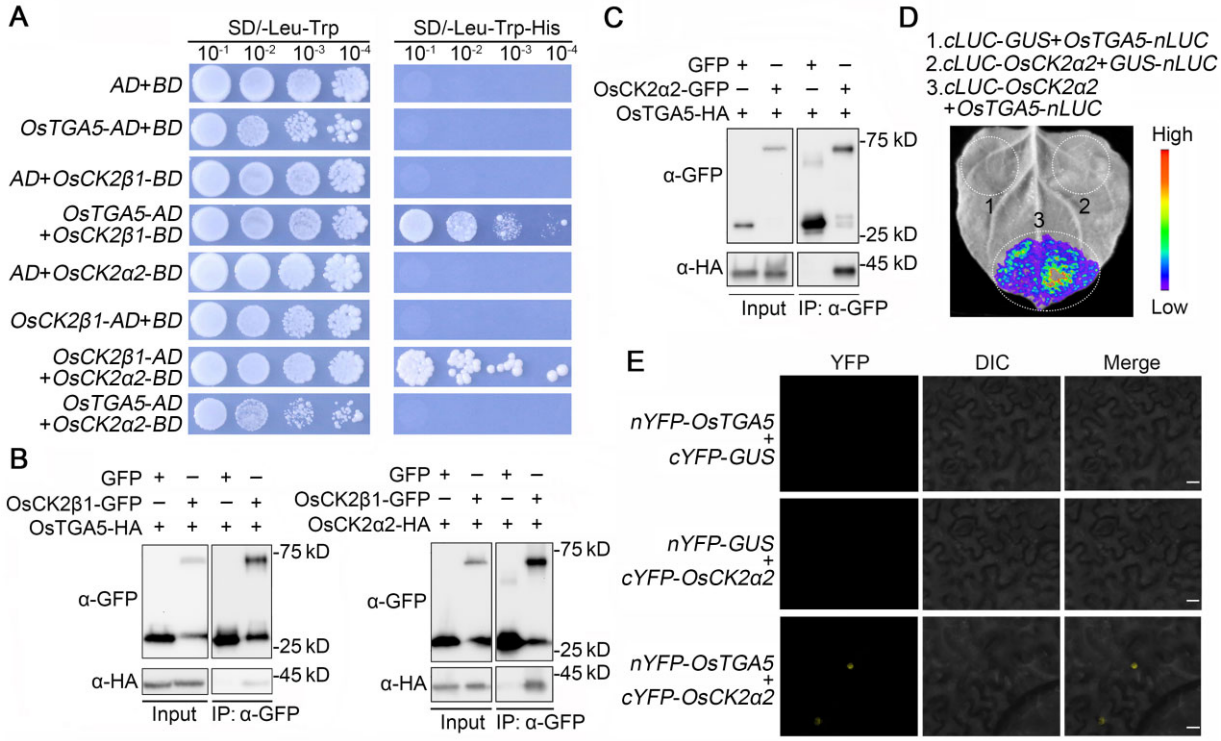

Figure 5 OsTGA5 interacts with the nuclear CK2 kinase complex. A, OsCK2β1 interacts with OsTGA5 and OsCK2α2, as shown by Y2H. The combinations with the empty vectors AD (pGADT7) or BD (pGBKT7) were used as negative controls. B, Determining the in vivo interaction between OsCK2β1 and OsTGA5, and OsCK2β1 and OsCK2α2 by co-IP assays via Agrobacterium-mediated transient expression in *N. benthamiana* leaves. The combinations of *OsCK2β1-GFP* and *OsTGA5-HA*, or *OsCK2β1-GFP* and *OsCK2α2-HA*, constructs were co-infiltrated in *N. benthamiana*; *OsTGA5-HA* or *OsCK2α2-HA* co-infiltrated with *GFP* served as negative controls. Proteins were extracted 3 d after infiltration, and IP was carried out with anti-GFP beads. Immunoblotting was conducted with anti-GFP and anti-HA antibodies. C–E, OsTGA5 and OsCK2α2 interact in vivo, as determined by co-IP, split-LUC complementation, and BiFC assays. C, *OsCK2α2-GFP* and *OsTGA5-HA* constructs were co-infiltrated in *N. benthamiana*; *OsTGA5-HA* co-infiltrated with *GFP* served as the negative control. D, Constructs encoding OsTGA5-nLUC (N-terminal half of LUC) and cLUC- OsCK2α2 (C-terminal half of LUC) were co-infiltrated in *N. benthamiana* leaves. Three days later, infiltrated leaves were detached and sprayed with 1 mM luciferin, and the bioluminescence images were captured by a CCD camera. The combinations *cLUC-GUS* + *OsTGA5-nLUC*, and *cLUC-OsCK2α2* + *GUS-nLUC* were co-infiltrated as the negative controls. E, Constructs encoding nYFP-OsTGA5 and cYFP-OsCK2α2 were co-infiltrated in *N. benthamiana* leaves. The combinations of constructs *nYFP-OsTGA5* + *cYFP-GUS*, and *nYFP-GUS* + *cYFP-OsCK2α2* were used as the negative controls. Three days after infiltration, YFP signals were observed using a confocal microscope. Scale bars = 20 μm.

Ostga5-1 at 48 versus 0 h appeared to be enriched into a single GO term (Figure 4C). Moreover, the upregulated genes in ZH11 were specifically enriched in pathways related to regulation of catalysis, monooxygenase, and electron carrier activities (Figure 4C, highlighted by blue dots). In contrast, the upregulated genes in *Ostga5-1* at 48 versus 0 h were specifically enriched in one GO term related to nucleotide binding (Figure 4C, highlighted by green dot), which contains 288 genes, including 26 genes encoding NBS-LRR proteins, 117 receptor-like kinase and seven *MAPK* genes, and 16 and 6 genes potentially involved in reduction–oxidation and calcium signaling pathways, respectively (Supplemental Data Set S1). The same 288 genes were also enriched for the biological processes of cell death and response to stress, as indicated by GO enrichment analyses (Supplemental Figure S8). Taken together, our transcriptome analyses suggest that upon blast fungus invasion, OsTGA5 suppresses the transcription of multiple genes with potential functions in various immune-related signaling pathways.

OsTGA5 interacts with the nucleus-localized CK2 kinase complex

To further investigate the regulatory mechanism behind OsTGA5-mediated rice immunity, we turned to OsTGA5-binding proteins by screening a rice cDNA library via yeast two-hybrid (Y2H) assays. We thus identified the regulatory β subunit of the nucleus-localized CK2 kinase complex OsCK2β1 (Chen et al., 2015) as a candidate partner of OsTGA5 (Figure 5A and Supplemental Figure S9). We validated the interaction between OsCK2β1 and OsTGA5 in vivo by co-immunoprecipitation (co-IP) assays with an antibody against the green fluorescent protein (GFP) in total protein extracts from *Nicotiana benthamiana* leaves transiently co-expressing *OsTGA5-HA* and *OsCK2β1-GFP* (Figure 5B, left). Sequencing revealed that ZH11, like Nipponbare, carries a premature stop codon in *Hd6*. Thus, OsCK2α2 is the unique catalytic subunit specifically localizing to the nucleus (Supplemental Figure S9). We performed Y2H and co-IP assays to determine whether OsCK2α2 and

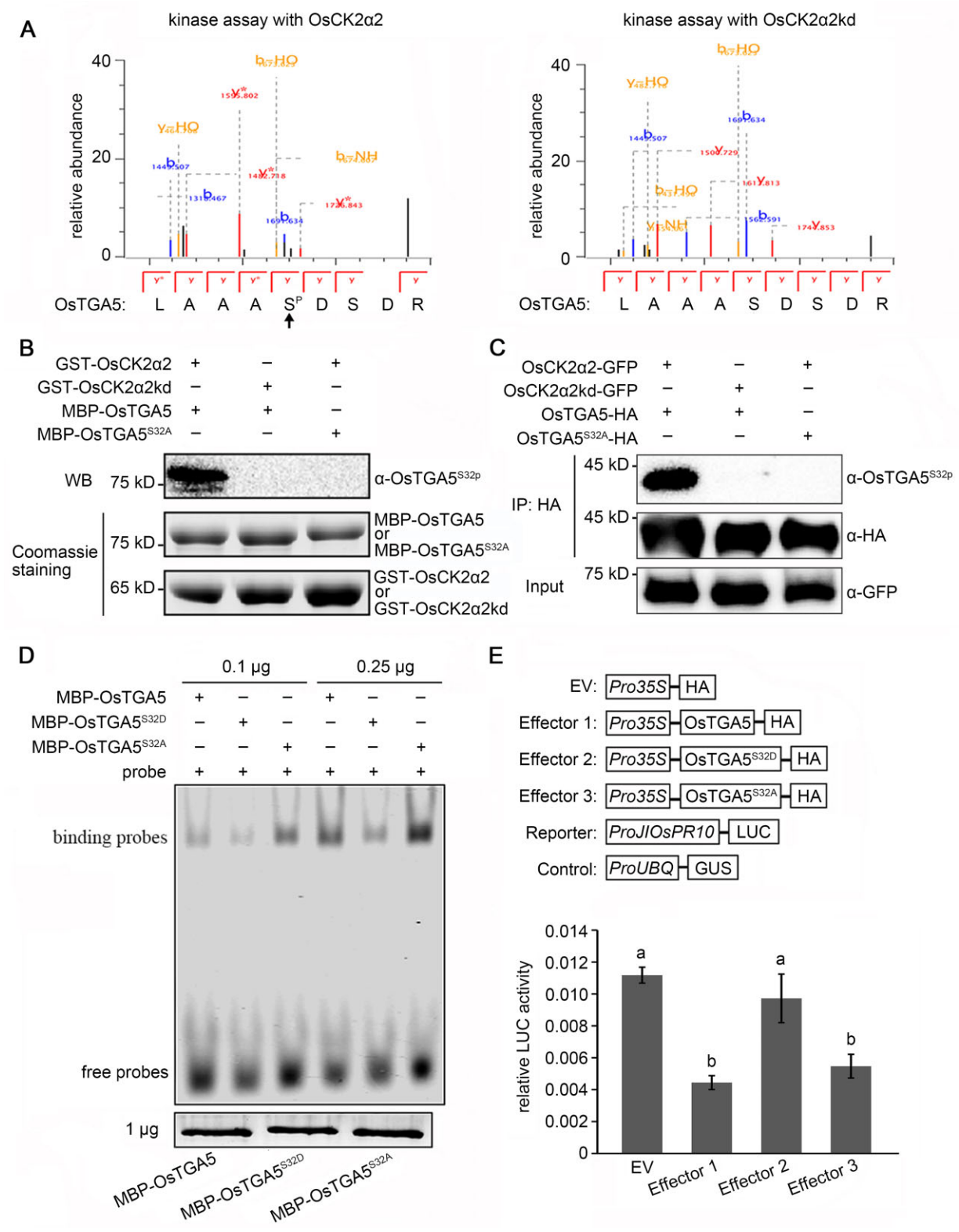

Figure 6 OsCK2α2 phosphorylates OsTGA5 at Ser32 and compromises its DNA binding ability and suppression on *JIOsPR10* transcription. A, Identification of the OsTGA5 residue phosphorylated by OsCK2α2 via mass spectrometry analysis. The in vitro kinase assays were performed with recombinant GST-OsCK2α2 and MBP-OsTGA5; the kinase-deficient form GST-OsCK2α2kd was used as a negative control. Annotated spectra for the phosphorylated peptide of OsTGA5 are shown at the bottom with "p" indicating the phosphorylation site (indicated by an arrow). B, OsCK2α2 phosphorylates OsTGA5 at S32 in vitro. The kinase assays were carried out with the indicated recombinant proteins, followed by immunoblotting with an antibody specifically recognizing phosphorylated S32 of OsTGA5 (OsTGA5^{S32p}). The S32A mutation (nonphosphorylatable, OsTGA5^{S32A}) was introduced to verify the specificity of the antibody against OsTGA5^{S32p}. The amount of recombinant proteins are shown by Coomassie blue staining. C, S32 of OsTGA5 can be phosphorylated by OsCK2α2 in planta. Total proteins were extracted from *N. benthamiana*

(Continued)

OsCK2β1 can form a complex. Indeed, OsCK2α2 is associated with OsCK2β1 both in yeast and in planta (Figure 5, A and B). We also tested whether OsCK2α2 can interact with OsTGA5, and found no direct binding between them in yeast (Figure 5A). However, we observed a positive in vivo interaction between OsCK2α2 and OsTGA5 via co-IP, split-LUC complementation and bimolecular fluorescence complementation (BiFC) assays; in particular, BiFC revealed that OsCK2α2 and OsTGA5 interact in the nucleus (Figure 5, C–E). Therefore, OsTGA5 associates with the nucleus-localized CK2 complex by directly binding to the β subunit.

OsCK2α2-mediated phosphorylation of OsTGA5 at Serine 32 reduces its DNA-binding ability and suppression of *JIOsPR10* transcription

The β subunit of the CK2 kinase complex usually mediates substrate recognition of the CK2 complex (Mulekar and Huq, 2014), which prompted us to investigate whether OsCK2α2 can phosphorylate OsTGA5. Lysine 63 (K63) in OsCK2α2 is the conserved amino acid essential for ATP binding and for kinase activity. To test whether the CK2 complex phosphorylates OsTGA5, we generated a kinase-deficient variant of OsCK2α2 (OsCK2α2kd) with K63 mutated to arginine (R) as a negative control for the kinase assay. We incubated purified recombinant MBP-OsTGA5 for an in vitro kinase assay together with glutathione *S*-transferase (GST)-OsCK2α2 or GST-OsCK2α2kd, followed by mass spectrometry analysis of MBP-TGA5 to identify phosphorylation site(s). We established that serine (S) 32 of OsTGA5 is the unique site being phosphorylated by OsCK2α2 (with 100% confidence), but not by OsCK2α2kd (Figure 6A). The S32 residue is conserved among TGA members within clade II of the D subgroup in rice and Arabidopsis (Supplemental Figure S10).

To confirm the phosphorylation of OsTGA5 by OsCK2α2, we produced a polyclonal antibody specifically recognizing OsTGA5 phosphorylated at S32 (OsTGA5^{S32p}). Immunoblotting with the anti-OsTGA5^{S32p} antibody following in vitro kinase assays with the recombinant proteins showed that the S32 phosphorylation signal could be detected when recombinant OsTGA5 was incubated with OsCK2α2, but not with OsCK2α2kd (Figure 6B). Similarly, we failed to detect any phosphorylation signal when recombinant OsTGA5^{S32A}, in which S32 was mutated to a non-phosphorylatable alanine (A) residue, was incubated with OsCK2α2 (Figure 6B). These data demonstrate that OsCK2α2 can phosphorylate OsTGA5 at S32 in vitro, which can be specifically recognized by the anti-OsTGA5^{S32p} antibody. Furthermore, to determine the in vivo phosphorylation of OsTGA5 by OsCK2α2, we transiently co-expressed OsTGA5-HA and OsCK2α2-GFP or OsCK2α2kd-GFP in *N. benthamiana* leaves. As a negative control, OsTGA5^{S32A}-HA and OsCK2α2-GFP were also co-expressed. We extracted total proteins from *N. benthamiana* leaves and subjected them to IP with an anti-HA antibody, followed by immunoblotting using the anti-OsTGA5^{S32p} antibody. We observed a strong S32 phosphorylation signal when OsTGA5 was co-expressed with OsCK2α2, whereas no signal was detected in the sample co-expressing OsTGA5 and OsCK2α2kd or the negative control (Figure 6C). Thus, OsTGA5 is phosphorylated at S32 by OsCK2α2 both in vitro and in vivo.

To further investigate the regulation of OsTGA5 activity by CK2 phosphorylation, we introduced the S32D mutation in OsTGA5 to generate a phosphomimic variant of the protein. We determined that as with OsTGA5, both OsTGA5^{S32D} and OsTGA5^{S32A} localize to the nucleus when their encoding constructs were transfected in rice protoplasts (Supplemental Figure S11A), indicating that the phosphorylation status at S32 does not affect OsTGA5 localization. Moreover, S32 phosphorylation had little influence on the interaction between OsTGA5 and NH1 (Supplemental Figure S11B). We then turned to EMSAs to investigate whether the phosphorylation status of OsTGA5 (OsTGA5, OsTGA5^{S32D}, and OsTGA5^{S32A}) affected its affinity for the binding motif within the *JIOsPR10* promoter. To remain in the linear range of the assay, we decreased the amount of recombinant OsTGA5 protein mixed with the probes from 5 (used for Figure 3B) to 0.1 μg, which was the smallest amount necessary to detect a clear electrophoresis mobility shift in this assay, and 0.25 μg. With both lower amounts of recombinant protein, we detected a clear mobility shift with OsTGA5; the intensity of the band decreased with recombinant OsTGA5^{S32D}, whereas OsTGA5^{S32A} exhibited the highest affinity for the DNA probe (Figure 6D). Therefore, phosphorylation of OsTGA5 at S32 decreases its affinity for DNA.

Given the effects of phosphorylation at the S32 residue in vitro, we wished to analyze whether effector constructs expressing *OsTGA5*, *OsTGA5*^{S32D}, or *OsTGA5*^{S32A} would show distinct regulation of the *JIOsPR10* transcription. We thus

Figure 6 (Continued)
leaves co-infiltrated with the indicated construct combinations and subjected to IP with anti-HA beads, followed by immunoblotting with the anti-OsTGA5^{S32p} antibody. Only when co-expressed with OsCK2α2-GFP but not OsCK2α2kd-GFP, OsTGA5-HA could be detected with a strong phosphorylation signal. When OsTGA5^{S32A}-HA was co-expressed with OsCK2α2-GFP, the phosphorylation band could not be detected. D, DNA affinity of OsTGA5, OsTGA5^{S32A}, and OsTGA5^{S32D} (carrying a S32D phosphomimic mutation) via EMSA. The DNA fragment of the *JIOsPR10* promoter containing the TGACGT motif was used as probe; the amount of recombinant OsTGA5 protein added in the assay is indicated on top. Equal loading of OsTGA5 proteins used in EMSA is shown in the Coomassie blue-stained gel. E, OsTGA5^{S32D} does not suppress the expression of the *LUC* reporter gene driven by the *JIOsPR10* promoter in ZH11 protoplasts. Top, schematic diagrams of the constructs used in this assay. Bottom, relative LUC activity of each combination of Reporter + Effector + Control transfected into protoplasts, calculated as luminescence/GUS activity. Data are means ± SE (n = 8). Different lowercase letters indicate significant differences ($P < 0.01$, one-way ANOVA). This assay was performed in three independent replicates with similar results.

transfected rice protoplasts with each effector construct and the *LUC* reporter construct (Reporter from Figure 3C). Similar to *OsTGA5*, the transient overexpression of *OsTGA5*^{S32A} significantly decreased relative LUC activity compared with that obtained with the empty vector control ($P < 0.01$; Figure 6E). In contrast, protoplasts transfected with *OsTGA5*^{S32D} exhibited significantly higher relative LUC activity than those expressing *OsTGA5* or *OsTGA5*^{S32A}, indicating that repression of *JIOsPR10* transcription by OsTGA5 is compromised by phosphorylation at S32. Taken together, our results indicate that the phosphorylation at S32 by OsCK2α2 reduces OsTGA5 affinity to the *JIOsPR10* promoter, thereby alleviating the suppression of *JIOsPR10* transcription.

Ser32 phosphorylation alleviates the negative regulation of OsTGA5 over rice defense

To evaluate the contribution of OsTGA5 phosphorylation at S32 in rice resistance against blast fungus, we created transgenic lines overexpressing *OsTGA5*, *OsTGA5*^{S32A}, or *OsTGA5*^{S32D} with an N-terminal FLAG tag in the *Ostga5-1* mutant background. We selected two lines for each construct from the T_1 generation (*Ostga5-1 FLAG-OsTGA5*-OE lines #1 and #16; *Ostga5-1 FLAG-OsTGA5*^{S32A}-OE lines #3 and #5; *Ostga5-1 FLAG-OsTGA5*^{S32D}-OE lines #18 and #20) with comparable and higher levels of *OsTGA5*, *OsTGA5*^{S32A}, or *OsTGA5*^{S32D} transcripts, respectively, for further analysis (Figure 7A). We first measured relative *JIOsPR10* transcript levels in ZH11, *Ostga5-1*, and the transgenic plants after *M. oryzae* inoculation. We observed that *OsTGA5* overexpression in the *Ostga5-1* background reduces *JIOsPR10* transcripts to levels lower than in ZH11 at 24 hpi, with *OsTGA5*^{S32A} overexpression resulting in even lower relative *JIOsPR10* transcript levels. However, relative *JIOsPR10* transcript levels were notably higher in the *Ostga5-1 FLAG-OsTGA5*^{S32D}-OE plants compared with *Ostga5-1 OsTGA5*-OE and *Ostga5-1 OsTGA5*^{S32A}-OE lines (Figure 7B), suggesting that in vivo phosphorylation of OsTGA5 at S32 alleviates its repression of *JIOsPR10* transcription.

We then challenged these transgenic plants with punch inoculations with Guy11 conidial spores. The transgenic plants overexpressing *OsTGA5* were more susceptible to the fungus than the wild-type ZH11 (Figure 7C). In agreement with the *JIOsPR10* transcript levels above, the *Ostga5-1 FLAG-OsTGA5*^{S32A}-OE lines showed increased susceptibility, compared with the *Ostga5-1 FLAG-OsTGA5*-OE plants, whereas the *Ostga5-1 FLAG-OsTGA5*^{S32D}-OE lines were significantly less susceptible than the *Ostga5-1 OsTGA5*-OE or *Ostga5-1 OsTGA5*^{S32A}-OE lines. Taken together, our data indicate that phosphorylation of OsTGA5 at S32 compromises OsTGA5 function as a negative regulator of *JIOsPR10* transcription and rice defense against blast fungus.

Furthermore, to determine the phosphorylation levels of OsTGA5 S32 before and after *M. oryzae* infection, we challenged the *Ostga5-1 FLAG-OsTGA5*-OE lines with Guy11 conidial spores by spraying and harvested the leaves before (0 hpi) and after (24 and 48 hpi) *M. oryzae* inoculation. We then performed immunoblotting assays with the anti-OsTGA5^{S32p} antibody after IP with an anti-FLAG antibody. We observed that both *Ostga5-1 FLAG-OsTGA5*-OE lines show higher phosphorylation of OsTGA5 at S32 at 48 hpi relative to 0 hpi (Figure 7D). Moreover, to investigate the influence of PTI activation on OsTGA5 phosphorylation at S32, we transiently expressed *OsTGA5-HA* in ZH11 protoplasts, which were then treated with chitin. As shown in Figure 7E, phosphorylation of OsTGA5 S32 was markedly enhanced 20 min after chitin treatment but returned to basal levels within 60 min. Thus, these results indicate that blast fungus invasion can promote the in vivo phosphorylation of OsTGA5 at S32.

Knockout of *OsCK2α2* compromises rice resistance against blast fungus

Consistent with the enhancement of OsTGA5 S32 phosphorylation by blast fungus infection, relative *OsCK2β1* transcript levels were dramatically induced by *M. oryzae* inoculation in ZH11, rising to over 100 times higher levels than in mock samples, whereas *OsCK2α2* transcripts levels only slightly increased upon inoculation (Figure 8A). Considering the possibility that the CK2α subunit may function without β subunit-mediated substrate recognition (Mulekar and Huq, 2014), we generated knockout mutants of *OsCK2α2* in ZH11 by CRISPR/Cas9 genome editing. We obtained three homozygous *Osck2α2* mutants from independent T_0 transgenic plants, all carrying single but different 1-bp insertions at the same position, which were named *Osck2α2-1*, *Osck2α2-2*, and *Osck2α2-3*, respectively (Figure 8B). When challenged with Guy11 by punch inoculation, all *Osck2α2* mutants displayed increased susceptibility compared with ZH11 (Figures 8C). The *Osck2α2-1* mutant was more susceptible to the *M. oryzae* isolate ZHONG1 as well (Supplemental Figure S4). In addition, we determined that both resting and *M. oryzae*-induced *JIOsPR10* transcript levels are significantly lower in the *Osck2α2* mutants than in ZH11 (Figure 8D); chitin-induced ROS burst and callose deposition were also attenuated in the absence of OsCK2α2 (Supplemental Figure S12). Furthermore, we assessed the in vivo phosphorylation of OsTGA5 S32 by transfecting the *OsTGA5-HA* construct in ZH11 and *Osck2α2-1* protoplasts. After treatment with chitin for 20 min, we detected OsTGA5 phosphorylation at S32 in ZH11, but not in *Osck2α2-1* protoplasts (Figure 8E), indicating that OsCK2α2 is required for the phosphorylation of OsTGA5 in rice.

To investigate whether the kinase activity of OsCK2α2 is essential for inducing *JIOsPR10* transcription and enhancing resistance against blast fungus, we overexpressed *OsCK2α2* and *OsCK2α2kd* in ZH11. As shown in Supplemental Figure S13, A and B, the T_1 transgenic plants overexpressing *OsCK2α2* displayed a dramatic upregulation of *JIOsPR10* transcript levels, but not those overexpressing *OsCK2α2kd*. Upon inoculation with *M. oryzae*, the *OsCK2α2*-OE plants showed greater resistance compared with ZH11 (Supplemental Figure S13C).

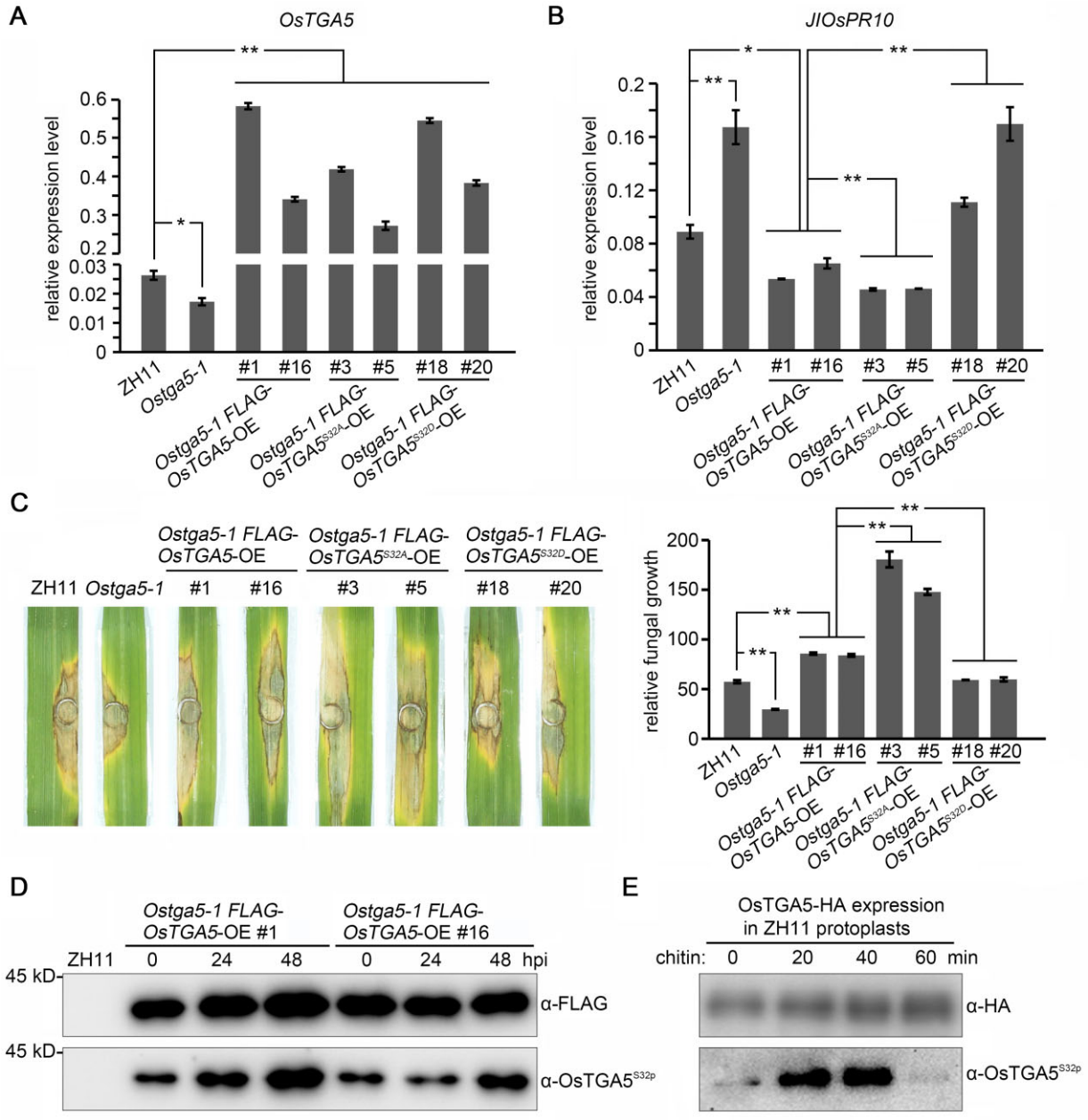

Figure 7 OsTGA5 Ser32 phosphorylation, promoted by *M. oryzae* invasion, alleviates the suppression of rice defense by OsTGA5. A and B, Relative transcript levels of *OsTGA5* (A) and *JIOsPR10* at 24 hpi (B) in ZH11, *Ostga5-1* and transgenic lines overexpressing *FLAG-OsTGA5* (#1 and #16), *FLAG-OsTGA5*^{S32A} (#3 and #5) and *FLAG-OsTGA5*^{S32D} (#18 and #20) in the *Ostga5-1* mutant background. *UBQ* was used as the internal control. Data are means ± SE (n = 3). Significant difference were determined by one-way ANOVA (*$P < 0.05$; **$P < 0.01$). These data are from one representative out of three independent experiments. C, Punch inoculation of leaves with Guy11 conidia, performed using 5-week-old ZH11, *Ostga5-1*, *Ostga5-1 FLAG-OsTGA5*-OE, *Ostga5-1 FLAG-OsTGA5*^{S32A}-OE, and *Ostga5-1 FLAG-OsTGA5*^{S32D}-OE plants. The diseased leaves were photographed at 9 dpi (left), and the fungal biomass of punch-inoculated leaves was determined (right). Data are means ± SE from three biological replicates. Significant differences were determined by one-way ANOVA (**$P < 0.01$). D, In vivo phosphorylation of OsTGA5 S32 is enhanced by blast fungus infection. Total proteins were extracted from ZH11 and *Ostga5-1 FLAG-OsTGA5*-OE (#1 and #16) plants before and after Guy11 inoculation by spraying, then subjected to IP assays with anti-FLAG beads and immunoblotting with the anti-OsTGA5^{S32p} antibody. Note the greater intensity of OsTGA5^{S32p} signals at 48 hpi. E, Phosphorylation of OsTGA5 S32 is promoted by chitin treatment. *OsTGA5-HA* was transiently expressed in ZH11 protoplasts. At different time points following treatment with 1 μM chitin, the signals of OsTGA5^{S32p} were detected by immunoblotting.

Interestingly, the plants overexpressing *OsCK2α2kd* were more susceptible than ZH11 (Supplemental Figure S13C), which may be attributed to the alteration of endogenous OsCK2α2 function by overexpressing its kinase-deficient form. Taken together, our data demonstrate that OsCK2α2, depending on its kinase activity, functions as a positive regulator of *JIOsPR10* transcription and immune responses against blast fungus.

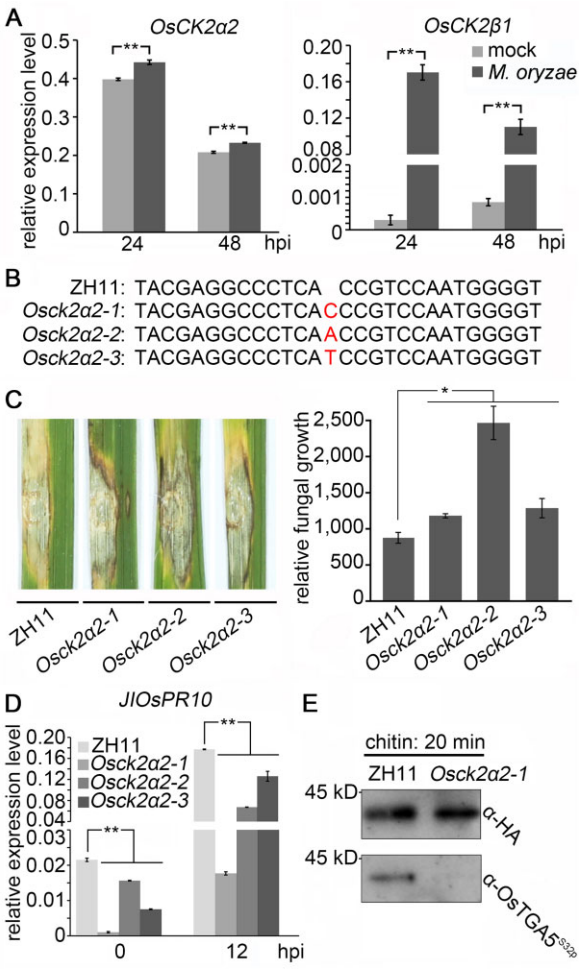

Figure 8 Knockout of *OsCK2α2* compromises rice resistance against blast fungus. A, Relative transcript levels of *OsCK2α2* and *OsCK2β1* in ZH11 at different time points after spray-inoculation with Guy11 conidia. Water containing 0.02% Tween-20 was used as the mock control. *UBQ* served as the internal control. Data are means ± SE ($n = 3$). Significant differences were determined by one-way ANOVA (**$P < 0.01$). These data are from one representative out of three independent experiments. B, Mutation sites of homozygous *Osck2α2* mutants generated via CRISPR/Cas9 gene editing in ZH11. C, Four-week-old plants of ZH11 and *Osck2α2* mutants were punch-inoculated with Guy11 conidia. The diseased leaves were photographed at 8 dpi (left). Fungal biomass of punch-inoculated leaves was determined (right). Data are means ± SE from three biological replicates. Significant differences were determined by one-way ANOVA (*$P < 0.05$). D, Relative transcript levels of *JIOsPR10* in ZH11 and *Osck2α2* mutants before and after inoculation with *M. oryzae*. *UBQ* was used as the internal control. Data are means ± SE ($n = 3$). Significant differences were determined by one-way ANOVA (**$P < 0.01$). The data are from one representative out of three independent experiments. E, OsTGA5 is not phosphorylated upon chitin treatment in the *Osck2α2-1* mutant. *OsTGA5-HA* was transiently transfected in ZH11 and *Osck2α2-1* protoplasts. Following treatment with 1 μM chitin for 20 min, OsTGA5 S32 phosphorylation was analyzed by immunoblotting with the anti-OsTGA5^{S32p} antibody.

Discussion

In this study, we demonstrated that OsTGA5 plays a negative role in rice immune responses against blast fungus. Following *M. oryzae* invasion, the loss of OsTGA5 led to greater accumulation of SA. Moreover, chitin-induced ROS burst and callose deposition were also enhanced in the *Ostga5* mutant. Both OsTGA5 and rTGA2.1 negatively regulate rice immunity. However, perturbing the function of rTGA2.1 results in increased rice resistance to *Xoo* with a developmental cost, such as dwarfing and reduced tiller numbers (Fitzgerald et al., 2005). It is worth noting here that the *Ostga5* mutants generated in this study displayed increased resistance to blast fungus with no obvious growth or development penalty, suggesting the potential of utilizing *OsTGA5* alteration in rice resistance breeding.

OsTGA5 binds to the TGACGT motif in the *JIOsPR10* promoter and suppresses its transcription. Furthermore, our RNA-seq analyses shed light on the repression imposed by OsTGA5 on the transcription of multiple defense-related genes in various signaling pathways. TGA2 in Arabidopsis possesses a parallel basic function in repressing *PR1* expression, whereas it acts as a positive regulator of *PR1* in the *tga5 tga6* double mutant (Kesarwani et al., 2007), implying that the specific regulatory function of AtTGA2 is complex and can vary due to its interplay with other TGA members. AtTGA2 suppresses *PR1* transcription by forming an oligomer that sits on its cognate binding site within the *PR1* promoter and hinders transcription (Boyle et al., 2009). Whether OsTGA5 functions in a similar way to repress its target genes still needs to be explored.

Although previous studies have indicated that CK2 controls plant virus propagation (Hung et al., 2014; Hu et al., 2015), its role in plant immune responses against fungal pathogens is still ambiguous. In tobacco, SA increases the activity of nuclear CK2, and treatment with a CK2 inhibitor impairs transcription of a *GUS* reporter gene driven by the *as-1* element (Hidalgo et al., 2001), suggesting a role for nuclear CK2α in inducing the transcription of TGA-targeted genes. A later study with elaborate biochemical assays showed that Ser-11, Thr-12, and Thr-16 of Arabidopsis TGA2 are possible phosphorylation sites by CK2, with the phosphorylation being enhanced by SA, although a truncated form of TGA2 lacking the first 20 amino acids can still be phosphorylated by CK2 in Arabidopsis leaf extracts (Kang and Klessig, 2005). Moreover, the DNA affinity of Arabidopsis TGA2 was attenuated by CK2, but the phosphorylation of Ser-11, Thr-12, and Thr-16 did not contribute to this regulation (Kang and Klessig, 2005), implying that additional CK2-phosphorylating site(s) exist and are involved in impairing TGA2 binding to DNA. Our study reveals a mechanism by which TGA activity in regulated by CK2 in rice: the unique nuclear CK2 α subunit in typical *japonica* rice cultivars phosphorylates OsTGA5 at S32 and alleviates its transcriptional suppression of downstream defense genes by decreasing OsTGA5 affinity to its binding DNA sequence. Our results add a positive role for CK2 in mediating plant defense against fungal pathogens to the multiple biological processes it participates in.

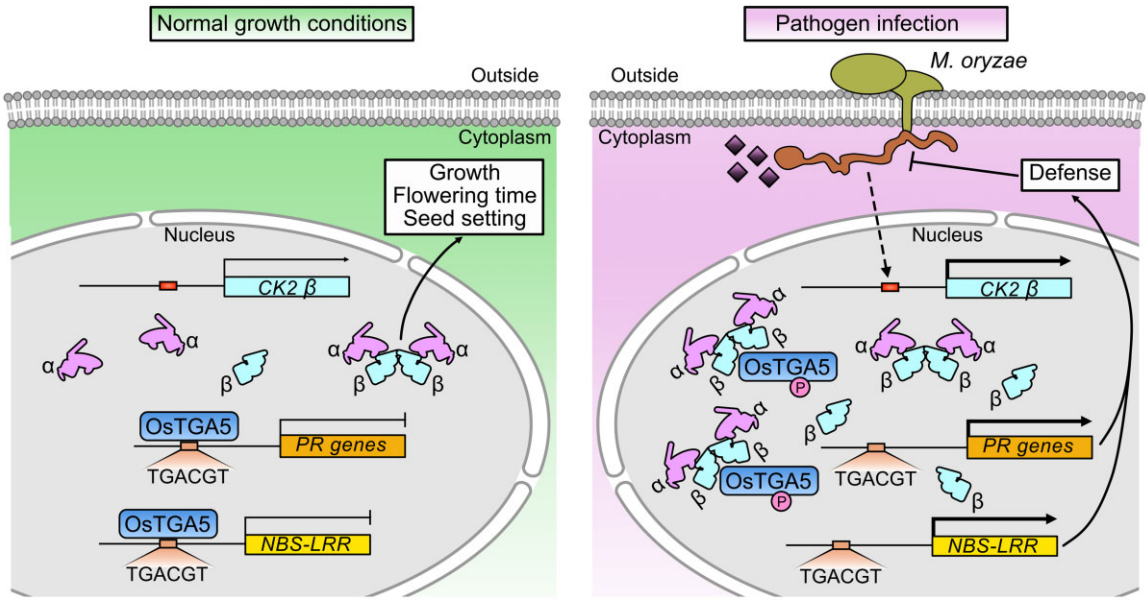

Figure 9 A working model of the regulation of OsTGA5 activity by nuclear CK2 upon *M. oryzae* invasion. Without blast fungus infection, OsTGA5 suppresses the transcription of its downstream defense-related genes by binding to their promoters. Following blast fungus invasion, dramatically increased *CK2*β expression promotes CK2 complexes to interact with and phosphorylate OsTGA5, which in turn releases OsTGA5 from its target promoters, induces the transcription of defense-related genes, and activates rice defense responses against *M. oryzae*.

Upon nuclear enrichment of NPR1 promoted by higher endogenous SA levels in Arabidopsis, the BTB/POZ domain of NPR1 interacts with the N-terminal repression domain of TGA2, which in turn disassembles the TGA2 oligomer and attenuates its repression of target genes (Boyle et al., 2009). The S32 residue is located in the homologous repression domain of OsTGA5, but its phosphorylation did not affect the interaction between OsTGA5 and NH1. In addition, in contrast to Arabidopsis, rice plants accumulate continuously high SA levels during normal growth, which exhibit little change after pathogen infection (Yang et al., 2013). Thus, SA does not appear to be the initial signal to impair the activity of OsTGA5 as a transcriptional repressor. In this case, phosphorylation of OsTGA5 by CK2 may act as a critical switch to elicit the expression of defense-related genes upon blast fungus invasion. In agreement, our results indicate that the in vivo phosphorylation of OsTGA5 at S32 is indeed enhanced by blast fungus inoculation and chitin treatment. Different from the overexpression of *OsTGA5* or *OsTGA5*^{S32A}, *Ostga5-1 OsTGA5*^{S32D}-OE lines were not more susceptible than the wild-type, which further suggests that CK2-dependent phosphorylation of OsTGA5 S32 compromises the suppressing role of OsTGA5 in rice immunity.

Taken together, we propose a working model to illustrate the molecular switch controlling OsTGA5 activity by nuclear CK2 during the activation of rice defense against blast fungus (Figure 9). Under normal growth conditions, OsTGA5 binds to the promoters of defense-related genes and suppresses their transcription to maintain a proper energy balance, so that nuclear CK2 is mainly engaged in regulating rice growth and development. Upon blast fungus invasion, increased expression of the *CK2*β subunit gene promotes the association between CK2 and OsTGA5, leading to enhanced phosphorylation of OsTGA5 at S32. Subsequently, phosphorylated OsTGA5 is released from the promoters of its target genes, and the transcription of defense-related genes is induced. Nevertheless, during the interaction between rice and blast fungus, other signaling pathway(s) may also exist to enhance the phosphorylation of OsTGA5 by CK2, which awaits to be determined through further studies.

Materials and methods

Plant materials and growth conditions

The generation of the knockout mutants for *OsTGA5* and *OsCK2*α*2* in the ZH11 background was conducted via CRISPR/Cas9 gene editing as described (Wang et al., 2015). The sgRNA target sequences for *OsTGA5* and *OsCK2*α*2* were 5′-ccaactgatgtcaaggtgcaca-3′ and 5′-ccctcaccgtccaatgggggtg-3′, respectively. To obtain transgenic plants overexpressing *OsTGA5*/*OsTGA5*^{S32A}/*OsTGA5*^{S32D} and *OsCK2*α*2*/*OsCK2*α*2kd*, their respective coding sequences were cloned into a binary vector with the maize *UBQ* promoter and the *Neomycin phosphotransferase II* selection marker and pCXUN-HA vector with the maize *UBQ* promoter and the *Hygromycin phosphotransferase* selection marker. The resulting constructs were transformed into *Ostga5-1* and ZH11, respectively. Primer sequences used for cloning the coding sequences by PCR can be found in Supplemental Table S3. The germinated rice seeds were grown in a chamber (Conviron, Winnipeg, Canada ; PGC20) at 28°C with a 12-h light (600–800 μmol/m^2/s)/12-h dark cycle and 70% humidity.

Blast fungus inoculation

The rice blast fungus isolates, Guy11 and ZHONG1, precultured on CMII medium, were grown on rice bran medium for 10 days in the dark at 25°C. After the aerial hyphae were flatten off, the growth plates were incubated under light (200–400 μmol/m^2/s, 12-h light/12-h dark cycle) for sporulation. The conidial spores were collected in water with 0.02% (v/v) Tween-20. Spraying and punch inoculation were carried out with 3- and 5-week-old rice plants, respectively, using the method previously described (Tian et al., 2020). Measuring the fungal biomass in the punch-inoculated leaf tissues was performed as described previously (Park et al., 2012). Two punched leaves detached from different plants were collected as one biological replicate. Leaf sheath inoculation was performed with about 30-day-old plants following the method described previously (Tian et al., 2020).

ROS assay and callose deposition

The ROS burst assay was performed as described previously (Tian et al., 2020). In brief, rice leaf discs of 7-day-old seedlings were cut and suspended in 100 μL water in a 96-well plate overnight. To detect ROS production, water was replaced with 100 μL reaction solution (20 μM luminol and 2.5 μg/mL peroxidase) containing 400 nM chitin (hexa-*N*-acetylchitohexaose). Time-dependent quantification of ROS production was recorded on a Mithras luminometer (Berthold) every 2 min for 1 h. Sixteen replicates were performed for each sample. For observing and quantifying chitin-induced callose deposition, the leaves of 7-day-old seedlings were detached and incubated with 400 nM chitin. The assay was performed as described previously (Yang et al., 2019). The callose deposits were observed using UV light (excitation 405 nm, emission 498 nm; Zeiss LSM880). The numbers of deposits were counted according to all fields of vision using ImageJ version 1.43U software (Schneider et al., 2012).

Measurement of SA and JA contents

For measuring endogenous SA and JA levels, 3-week-old seedlings of ZH11 and *Ostga5-1* were sprayed with Guy11 conidial spore suspension (2×10^5 spores/mL), with water spraying as the mock treatment. The leaf tissues from six plants were harvested as one biological replicate. The extraction and quantification of SA and JA were carried out according to the manufacturer's instructions (Wuhan Metware Biotechnology Co., Ltd., Wuhan, China), using the method previously described (He et al., 2020).

SA inhibitor AIP treatment

Three-week-old rice seedlings were treated with 30 μM AIP (BIOBOMEI, Hefei, China; AT6923) by spraying or with water as a mock control 24 h before inoculation with Guy11 conidial spores. At 4 dpi, the average number of disease lesions per leaf was calculated by counting the lesions on the most seriously diseased leaves of three individual plants.

RT-qPCR

Total RNA was extracted using the TRIzol reagent (CWBIO, Beijing, China; CW0580S) from leaf tissues, and 2 μg RNA was subjected to first-strand cDNA synthesis using EasyScript One-Step gDNA Removal and cDNA Synthesis SuperMix (TransGen, Beijing, China; AE311). qPCR was then performed using the PerfectStart Green qPCR SuperMix (TransGen, AQ601) on a CFX connect Real-time system (Bio-Rad, Hercules, California, USA). *UBQ* was used as the internal control. Sequences of the primers for amplifying the plant defense-related genes are provided in Supplemental Table S3.

Transcriptome deep sequencing and data analysis

Seven to eight 3-week-old ZH11 or *Ostga5-1* plants were collected at each time point as one biological replicate, and the RNA-seq analysis was performed on two biological replicates. Total RNA was extracted from the leaf tissues of ZH11 and the *Ostga5-1* mutant before and after Guy11 inoculation. The preparation and sequencing of the libraries were carried out at the Novogene Bioinformatics Institute (Beijing, China) as described previously (Zhang et al., 2017) with minor modifications. Briefly, total RNA was treated with DNase I to completely remove genomic DNA contamination, then purified using oligo poly(T) conjugated to magnetic beads. cDNA was synthesized and selected by size (370–420 bp) using AMPure XP system (Beckman Coulter, Beverly, California, USA) for mRNA-seq library construction. The final library was quality-controlled and paired-end sequenced on an Illumina platform (NovaSeq 6000) with a read length of 150 bp.

For data analysis, the raw reads were trimmed using Trimmomatic (version 0.39) to remove primer/adapter contamination and reads with poor quality. Paired-end clean reads were aligned to the *japonica* Nipponbare reference genome (MSU 7.0) using Hisat2. The mapped reads from each sample were assembled by StringTie (version 1.3.4d). FeatureCounts (version 1.6.4) was used to count the read number mapped to each gene. The Fragments Per Kilobase of transcript per Million mapped reads values of each gene were then calculated based on the length of the gene and read counts mapped to the corresponding gene. DEGs between two conditions/groups (two biological replicates per condition) were determined using the DESeq2 R package (version 1.30.1). Genes with a P-adj < 0.05 and $|\text{Log2(fold-change)}| > 1$ were defined as differentially expressed. Biological processes, cellular components, and molecular functions of DEGs were determined by GO term enrichment analysis Toolkit and Database for Agricultural Community (AgriGo version 2.0, http://systemsbiology.cpolar.cn/agriGOv2/). Go terms with P-value < 0.05 were considered as significant GO terms.

Y2H assay

The coding sequence of *OsTGA5* was cloned into the bait vector pGBKT7. The Matchmaker Gold Y2H system (Clontech, Mountain View, California, USA, 630489) carrying a rice cDNA library was used to screen for OsTGA5-

interacting proteins. Yeast strain AH109 was transformed and screened for positive clones, which were then sequenced to identify the putative interactors. For Y2H assay, the coding sequences of *OsTGA5*, *OsCK2α2*, and *OsCK2β1* were amplified by PCR using gene-specific primers (Supplemental Table S3) and cloned into pGADT7 or pGBKT7 (Clontech) as indicated. The appropriate pairs of constructs were transformed into yeast strain AH109. The yeast clones were grown on synthetic defined (SD) medium lacking Trp and Leu (SD −Trp −Leu) at 30°C for 2 days and then spotted onto SD medium lacking Trp, Leu, and His (SD −Trp −Leu −His) or SD −Trp −Leu −His −Ade to detect interactions.

Split-LUC complementation assay

The coding sequences of *OsTGA5*, *OsCK2α2*, and *OsCK2β1* were cloned into nLUC or cLUC vector (Chen et al., 2008) as indicated. The resulting constructs were then transiently co-expressed in *N. benthamiana* leaves via Agrobacterium (*Agrobacterium tumefaciens*, strain GV3101)-mediated infiltration, with agrobacteria resuspended (final OD600 = 0.6) in infiltration buffer (10 mM $MgCl_2$, 10 mM MES, 200 mM acetosyringone, pH 5.6). Three days postinfiltration, 1 mM D-luciferin was sprayed onto detached leaves, which were then kept in the dark for 5–10 min. LUC activity was detected using the LB985 NightSHADE plant imaging system (Berthold, Germany).

BiFC assay

The coding sequences of *OsTGA5* and *OsCK2α2* were cloned into pSY736 (with N-terminal nYFP) and pSY735 vectors (with N-terminal cYFP), respectively. The resulting expression cassettes were then individually transferred to the vector pMDC32. The final constructs were introduced in Agrobacterium (strain GV3101) for transient expression in *N. benthamiana* leaves. The YFP signals were detected using a confocal microscope (Zeiss LSM880) with excitation 514 nm, emission 570 nm.

co-IP assay in *N. benthamiana*

To perform the co-IP assays, the *N. benthamiana* leaves were detached 3 days after Agrobacterium-mediated infiltration and ground in liquid nitrogen. Total protein was extracted in extraction buffer (50 mM Tris–HCl pH 7.5, 150 mM NaCl, 1 mM EDTA, 1 mM DTT, 1% [v/v] IGEPAL CA-630, 10% [v/v] glycerol, 1 mM PMSF, 1× protease inhibitor cocktail). The protein samples were incubated with 10 μL GFP-Nanoab-Agarose beads (Lablead, Beijing, China; GNA-20-400) at 4°C for 2 h with gentle shaking. The beads were washed 4 times in washing buffer (same as extraction buffer but with 0.3% [v/v] IGEPAL CA630) and finally resuspended in 60 μL washing buffer. The samples were separated by SDS-PAGE and analyzed by immunoblotting using anti-GFP (TransGen, HT801, 1:1,000 dilution) and anti-HA (Abmart, Shanghai, China; 26D11, 1:5,000 dilution) antibodies with anti-mouse secondary antibody (Abbkine, Wuhan, China; A21010, 1:10,000 dilution). The primers used for the constructions are shown in Supplemental Table S3.

Preparation of rice protoplasts for subcellular localization observation and protein extraction

Rice protoplasts were released from young ZH11 etiolated seedlings. The protoplast preparation and polyethylene glycol-mediated transfection was performed as described previously (Trinidad et al., 2021) with minor modifications. In brief, after transfection, protoplasts were resuspended in W5 buffer (154 mM NaCl, 125 mM $CaCl_2$, 5 mM KCl, 5 mM glucose, 2 mM MES, pH 5.7) and then incubated at 28°C for 16 h. For subcellular localization work, the coding sequences of *OsCK2α2*, *OsCK2β1*, *OsTGA5*, $OsTGA5^{S32D,}$ and $OsTGA5^{S32A}$ were cloned into pYBA1132 vector (adding a GFP tag at the C terminus). The GFP signal was detected 16 h after transfection using a confocal microscope (Zeiss LSM880) with excitation 488 nm, emission 546 nm. For the IP and immunoblotting assays with protein samples extracted from rice protoplasts, the extraction buffer and washing buffer were the same as those used for the above co-IP assay.

Recombinant protein production and purification

The coding sequences of *OsTGA5*, $OsTGA5^{S32D}$, and $OsTGA5^{S32A}$ were cloned into the pMAL-c2G vector (adding a MBP tag at the N terminus), and the *OsCK2α2* coding sequence was cloned into pGEX-4T-1 vector (adding a GST tag at the N terminus). The fusion proteins were produced in *Escherichia coli* strain BL21(DE3) (induced with 0.5 mM IPTG at OD600 = 0.6 and grown at 18°C overnight). The recombinant proteins were purified according to the manufacturer's instructions. Amylose resin (BioLabs, Ipswich, Massachusetts, USA; E8021S) and glutathione resin (GE Healthcare, Chicago, Illinois, USA; 17075605) were used for purifying the recombinant MBP- and GST-tagged proteins, respectively.

In vitro kinase activity and mass spectrometry analysis

The in vitro kinase assay was performed as previously described (Kang and Klessig, 2005) with minor modifications. Briefly, 4 μg of purified GST-OsCK2α2 or GST-OsCK2α2kd combined with 2 μg of purified MBP-OsTGA5 was incubated in a 40-μL reaction mixture (50 mM Tris–HCl, pH 7.5, 10 mM $MgCl_2$, 50 mM KCl, 1 mM DTT, and 100 μM ATP) for 30 min at 30°C. The reaction components were separated by SDS-PAGE. After Coomassie blue staining, the MBP-OsTGA5 bands were excised and digested with trypsin. The phosphopeptides were enriched with solvent A (water with 0.1% [v/v] formic acid) and subjected to liquid chromatography-tandem mass spectrometry (LC–MS/MS) analysis as described before (Liu et al., 2017).

Detection of in vivo phosphorylation

A polyclonal antibody specifically recognizing phosphorylated Serine 32 of OsTGA5 ($OsTGA5^{S32p}$) was produced by

Abmart (Shanghai, China) using the phosphopeptide ALAAASpDSDRS as antigen. The phosphospecific antibody was further purified using an affinity column conjugated with the phosphorylated and nonphosphorylated peptides. To detect the phosphorylation of OsTGA5 S32 by OsCK2α2 in planta, the combinations of constructs *OsTGA5-HA* + *OsCK2α2-GFP*, *OsTGA5-HA* + *OsCK2α2kd-GFP*, and *OsTGA5*^{S32A}*-HA* + *OsCK2α2-GFP* were co-infiltrated in *N. benthamiana* leaves by Agrobacterium-mediated infiltration. Total proteins from each sample were extracted as above for co-IPs with *N. benthamiana* samples and immunoprecipitated with 10 μL anti-HA agarose beads (Abmart, M20013M). Immunoblotting was then performed with anti-HA and anti-OsTGA5^{S32p} antibodies (1:1,000 dilution). Anti-rabbit secondary antibody (Abbkine, A21020, 1:10,000 dilution) was used for anti-OsTGA5^{S32p} antibody.

Electrophoretic mobility shift assay

A 39-bp DNA fragment of the *JIOsPR10* promoter containing the TGACGT sequence or its mutated version was synthetized with Cy5 end-label as probes; sequences are provided in Supplemental Table S3. The probes were incubated with the indicated amount of recombinant OsTGA5 protein in a 20-μL reaction (100 mM Tris–HCl, pH 7.5, 100-mM KCl, 50-mM $MgCl_2$, 1-mM DTT, 0.05-mg/mL poly [dI-dC]) at 4°C for 30 min. For detecting the shift in mobility, a native polyacrylamide gel containing 3.5% (w/v) acrylamide was prerun in 0.5× Tris borate EDTA running buffer for 1 h at 4°C in the dark. The protein–DNA mixtures were then loaded and separated by electrophoresis for 1 h at 4°C with voltage 100 V. Images were captured with an Odyssey CLx Infrared Imaging System (LI-COR Biosciences, Lincoln, Nebraska, USA).

Transcriptional activity in rice protoplasts

The coding sequences of *OsTGA5*, *OsTGA5*^{S32D}, and *OsTGA5*^{S32A} were cloned into the pYBA1143 vector (adding a HA tag at the C terminus) to generate the effector constructs. The *GUS* reporter gene driven by the *UBQ* promoter was used as the transfection control. The 2,022-bp *JIOsPR10* promoter fragment upstream from the TSS was cloned into the pUC-LUC vector to drive *LUC* expression, to obtain the reporter construct. All primers used for plasmid construction are listed in Supplemental Table S3. The appropriate combinations of constructs were transfected into ZH11 protoplasts for transient expression. After 16 h, for each replicate, LUC activity was measured after adding D-luciferin and detected on a GloMax Navigator Microplate Luminometer (Promega, Madison, Wisconsin, USA). GUS signal was recorded with a BioTek citation five plate reader (Thermo Fisher Scientific, Waltham, MA, USA) after incubation with 20 μM MUG (Lablead, M1630) for 30 min at 37°C. The relative LUC activity was calculated by luminescence/GUS activity.

Rice protein extraction and IP assays

Total protein was extracted from rice leaves in the same extraction buffer as for *N. benthamiana* protein. The samples were incubated with 10 μL FLAG beads (Sigma-Aldrich, St. Louis, Missouri, USA; A2220-5ML) at 4°C for 2 h with gentle shaking, then immunoblotting was performed with anti-FLAG (Sigma-Aldrich; F1804, 1:5,000 dilution with anti-mouse secondary antibody) and anti-OsTGA5^{S32p} antibodies.

Statistical analyses

All statistical analyses were performed with one-way ANOVA and are provided in Supplemental Data Set S2.

Accession numbers

Sequence data from this article can be found in the EMBL/GenBank data libraries under accession numbers: *OsTGA5*, LOC_Os01g17260; *OsCK2α2*, LOC_Os07g02350; *OsCK2β1*, LOC_Os10g41520; *JIOsPR10*, LOC_Os03g18850; *OsPR1a*, LOC_Os07g03710; *OsWRKY45*, LOC_Os05g25770; *OsPR5*, LOC_Os12g43380; *OsCht1*, LOC_Os06g51060; *OsPR10b*, LOC_Os12g36850; *OsNAC4*, LOC_Os01g60020; and *UBQ*, LOC_Os03g13170. The RNA sequencing data have been deposited at the NCBI SRA database, under accession number PRJNA741871, which are publicly accessible at https://www.ncbi.nlm.nih.gov/bioproject/PRJNA741871.

Supplemental data

The following materials are available in the online version of this article.

Supplemental Figure S1. Phylogenetic tree showing the homology among the rice TGA members within clade II of the D subgroup and Arabidopsis TGA2.

Supplemental Figure S2. Mature panicles of ZH11 and the *Ostga5* mutants.

Supplemental Figure S3. Leaf sheath inoculation of ZH11 and *Ostga5-1* with Guy11 conidia.

Supplemental Figure S4. Punch inoculation of ZH11, *Ostga5-1*, and *Osck2α2-1* plants with *M. oryzae* isolate ZHONG1.

Supplemental Figure S5. JA levels in ZH11 and *Ostga5-1* with or without *M. oryzae* inoculation.

Supplemental Figure S6. The SA inhibitor AIP partially compromises the resistance of *Ostga5-1* against blast fungus.

Supplemental Figure S7. The transcriptional levels of *OsPR10b* and *OsNAC4* in ZH11 and *Ostga5-1* with or without *M. oryzae* inoculation.

Supplemental Figure S8. GO enrichment analyses of the specific upregulated genes in *Ostga5-1* at 48 hpi relative to 0 hpi.

Supplemental Figure S9. Subcellular localization of OsCK2α2 and OsCK2β1.

Supplemental Figure S10. Sequence alignment of the TGA members within clade II of the D subgroup in Arabidopsis and rice.

Supplemental Figure S11. Mutation of OsTGA5 S32 to D or A does not affect its nuclear localization or interaction with NH1.

Supplemental Figure S12. Chitin-induced PTI responses are compromised in the *Osck2α2-1* mutant.

Supplemental Figure S13. Overexpression of *OsCK2α2*, but not its kinase-deficient form, enhances *JIOsPR10* transcription and resistance against blast fungus.

Supplemental Table S1. Summary of the DEGs in *Ostga5-1* before and after Guy11 inoculation compared with ZH11.

Supplemental Table S2. List of the upregulated genes in *Ostga5-1* containing TGACGT in their promoters potentially involved in response to stress and stimulus.

Supplemental Table S3. Sequence of the primers used in this study.

Supplemental Data Set S1. List of the specifically upregulated genes in *Ostga5-1* 48 versus 0 h, compared with ZH11 48 versus 0 h.

Supplemental Data Set S2. ANOVA results.

Supplemental File S1. Text file of the alignment used to generate the phylogenetic tree in Supplemental Figure S1.

Supplemental File S2. The Newick format file of the tree in Supplemental Figure S1.

Acknowledgments

We thank Dr. Guo-Liang Wang (Department of Plant Pathology, Ohio State University) and Dr. Ying Wang (Department of Biological Sciences, Mississippi State University) for critical reading and suggestions on the manuscript.

Funding

This work was supported by the grants from the National Natural Science Foundation of China (Project Numbers: 31701777, U2005211, and 31972251).

Conflict of interest statement. The authors declare no conflict of interest.

References

Agrawal GK, Jwa NS, Rakwal R (2000) A novel rice (*Oryza sativa* L.) acidic PR1 gene highly responsive to cut, phytohormones, and protein phosphatase inhibitors. Biochem Biophys Res Commun **274**: 157–165

Alhoraibi H, Bigeard J, Rayapuram N, Colcombet J, Hirt H (2019) Plant immunity: the MTI-ETI model and beyond. Curr Issue Mol Biol **30**: 39–58

Boyle P, Su EL, Rochon A, Shearer HL, Murmu J, Chu JY, Fobert PR, Després C (2009) The BTB/POZ domain of the Arabidopsis disease resistance protein NPR1 interacts with the repression domain of TGA2 to negate its function. Plant Cell **21**: 3700–3713

Chen H, Zou Y, Shang Y, Lin H, Wang Y, Cai R, Tang X, Zhou JM (2008) Firefly luciferase complementation imaging assay for protein-protein interactions in plants. Plant Physiol **146**: 368–376

Chen J, Wang Y, Wang F, Yang J, Gao M, Li C, Liu Y, Liu Y, Yamaji N, Ma JF, et al. (2015) The rice CK2 kinase regulates trafficking of phosphate transporters in response to phosphate levels. Plant Cell **27**: 711–723

Chen K, Wang Y, Zhang R, Zhang H, Gao C (2019) CRISPR/Cas genome editing and precision plant breeding in agriculture. Ann Rev Plant Biol **70**: 667–697

Chisholm ST, Coaker G, Day B, Staskawicz BJ (2006) Host-microbe interactions: shaping the evolution of the plant immune response. Cell **124**: 803–814

Després C, DeLong C, Glaze S, Liu E, Fobert PR (2000) The Arabidopsis NPR1/NIM1 Protein Enhances the DNA Binding Activity of a Subgroup of the TGA Family of bZIP Transcription Factors. Plant Cell **12**: 279–290

Dodds PN, Rathjen JP (2010) Plant immunity: towards an integrated view of plant-pathogen interactions. Nat Rev Genet **11**: 539–548

Dröge-Laser W, Snoek BL, Snel B, Weiste C (2018) The Arabidopsis bZIP transcription factor family-an update. Curr Opin Plant Biol **45**: 36–49

Duan L, Liu H, Li X, Xiao J, Wang S (2014) Multiple phytohormones and phytoalexins are involved in disease resistance to *Magnaporthe oryzae* invaded from roots in rice. Physiol Plant **152**: 486–500

E ZG, Zhang YP, Zhou JH, Wang L (2014) Roles of the bZIP gene family in rice. Genet Mol Res **13**: 3025–3036

Fan W, Dong X (2002) In vivo interaction between NPR1 and transcription factor TGA2 leads to salicylic acid-mediated gene activation in Arabidopsis. Plant Cell **14**: 1377–1389

Fitzgerald HA, Canlas PE, Chern MS, Ronald PC (2005) Alteration of TGA factor activity in rice results in enhanced tolerance to *Xanthomonas oryzae* pv. *oryzae*. Plant J **43**: 335–347

Gatz C (2013) From pioneers to team players: TGA transcription factors provide a molecular link between different stress pathways. Mol Plant Microbe Interact **26**: 151–159

Hao Z, Wang L, Huang F, Tao R (2012) Expression of defense genes and antioxidant defense responses in rice resistance to neck blast at the preliminary heading stage and full heading stage. Plant Physiol Biochem **57**: 222–230

He Y, Zhao J, Yang B, Sun S, Peng L, Wang Z (2020) Indole-3-acetate beta-glucosyltransferase OsIAGLU regulates seed vigour through mediating crosstalk between auxin and abscisic acid in rice. Plant Biotechnol J **18**: 1933–1945

Hidalgo P, Garretón V, Berríos CG, Ojeda H, Jordana X, Holuigue L (2001) A nuclear casein kinase 2 activity is involved in early events of transcriptional activation induced by salicylic acid in tobacco. Plant Physiol **125**: 396–405

Hu Y, Li Z, Yuan C, Jin X, Yan L, Zhao X, Zhang Y, Jackson AO, Wang X, Han C, et al. (2015) Phosphorylation of TGB1 by protein kinase CK2 promotes barley stripe mosaic virus movement in monocots and dicots. J Exp Bot **66**: 4733–4747

Hung CJ, Huang YW, Liou MR, Lee YC, Lin NS, Meng M, Tsai CH, Hu CC, Hsu YH (2014) Phosphorylation of coat protein by protein kinase CK2 regulates cell-to-cell movement of Bamboo mosaic virus through modulating RNA binding. Mol Plant Microbe Interact **27**: 1211–1225

Jakoby M, Weisshaar B, Dröge-Laser W, Vicente-Carbajosa J, Tiedemann J, Kroj T, Parcy F (2002) bZIP transcription factors in Arabidopsis. Trends Plant Sci **7**: 106–111

Jwa NS, Agrawal GK, Rakwal R, Park CH, Agrawal VP (2001) Molecular cloning and characterization of a novel jasmonate inducible pathogenesis-related class 10 protein gene, JIOsPR10, from rice (*Oryza sativa* L.) seedling leaves. Biochem Biophys Res Commun **286**: 973–983

Kaneda T, Taga Y, Takai R, Iwano M, Matsui H, Takayama S, Isogai A, Che FS (2009) The transcription factor OsNAC4 is a key positive regulator of plant hypersensitive cell death. EMBO J **28**: 926–936

Kang HG, Klessig DF (2005) Salicylic acid-inducible Arabidopsis CK2-like activity phosphorylates TGA2. Plant Mol Biol **57**: 541–557

Katagiri F, Lam E, Chua NH (1989) Two tobacco DNA-binding proteins with homology to the nuclear factor CREB. Nature **340**: 727–730

Kesarwani M, Yoo J, Dong X (2007) Genetic interactions of TGA transcription factors in the regulation of pathogenesis-related genes and disease resistance in Arabidopsis. Plant Physiol **144**: 336–346

Kwon CT, Koo BH, Kim D, Yoo SC, Paek NC (2015) Casein kinases I and 2α phosphorylate *Oryza sativa* pseudo-response regulator 37 (OsPRR37) in photoperiodic flowering in rice. Mol Cells **38**: 81–88

Lefevere H, Bauters L, Gheysen G (2020) Salicylic acid biosynthesis in plants. Front Plant Sci **11**: 338

Liu Q, Wang Q, Deng W, Wang X, Piao M, Cai D, Li Y, Barshop WD, Yu X, Zhou T, et al. (2017) Molecular basis for blue light-dependent phosphorylation of Arabidopsis cryptochrome 2. Nat Commun **8**: 15234–15234

Lu SX, Liu H, Knowles SM, Li J, Ma L, Tobin EM, Lin C (2011) A role for protein kinase casein kinase2 α-subunits in the Arabidopsis circadian clock. Plant Physiol **157**: 1537–1545

Macho AP, Zipfel C (2014) Plant PRRs and the activation of innate immune signaling. Mol Cell **54**: 263–272

Mcgee JD, Hamer JE, Hodges TK (2001) Characterization of a PR-10 pathogenesis-related gene family induced in rice during infection with *Magnaporthe grisea*. Mol Plant Microbe Interact **14**: 877–886

Moon SJ, Park HJ, Kim TH, Kang JW, Lee JY, Cho JH, Lee JH, Park DS, Byun MO, Kim BG, et al. (2018) OsTGA2 confers disease resistance to rice against leaf blight by regulating expression levels of disease related genes via interaction with NH1. PLoS ONE **13**: e0206910

Mulekar JJ, Huq E (2014) Expanding roles of protein kinase CK2 in regulating plant growth and development. J Exp Bot **65**: 2883–2893

Park CH, Chen S, Shirsekar G, Zhou B, Khang CH, Songkumarn P, Afzal AJ, Ning Y, Wang R, Bellizzi M, et al. (2012) The *Magnaporthe oryzae* effector AvrPiz-t targets the RING E3 Ubiquitin Ligase APIP6 to suppress pathogen-associated molecular pattern-Triggered immunity in rice. Plant Cell **24**: 4748–4762

Rakwal R, Agrawal GK, Agrawal VP (2001) Jasmonate, salicylate, protein phosphatase 2A inhibitors and kinetin up-regulate OsPR5 expression in cut-responsive rice (*Oryza sativa*). J Plant Physiol **158**: 1357–1362

Salinas P, Fuentes D, Vidal E, Jordana X, Echeverria M, Holuigue L (2006) An extensive survey of CK2 alpha and beta subunits in Arabidopsis: multiple isoforms exhibit differential subcellular localization. Plant Cell Physiol **47**: 1295–1308

Schneider CA, Rasband WS, Eliceiri KW (2012) NIH Image to ImageJ: 25 years of image analysis. Nat Methods **9**: 671–675

Shimono M, Sugano S, Nakayama A, Jiang CJ, Ono K, Toki S, Takatsuji H (2007) Rice WRKY45 plays a crucial role in benzothiadiazole-inducible blast resistance. Plant Cell **19**: 2064–2076

Takahashi Y, Shomura A, Sasaki T, Yano M (2001) Hd6, a rice quantitative trait locus involved in photoperiod sensitivity, encodes the alpha subunit of protein kinase CK2. Proc Natl Acad Sci USA **98**: 7922–7927

Tian D, Yang F, Niu Y, Lin Y, Chen Z, Li G, Luo Q, Wang F, Wang M (2020) Loss function of SL (sekiguchi lesion) in the rice cultivar Minghui 86 leads to enhanced resistance to (hemi)biotrophic pathogens. BMC Plant Biol **20**: 507

Trinidad JL, Longkumer T, Kohli A (2021) Rice protoplast isolation and transfection for transient gene expression analysis. Methods Mol Biol **2238**: 313–324

Tsuda K, Katagiri F (2010) Comparing signaling mechanisms engaged in pattern-triggered and effector-triggered immunity. Curr Opin Plant Biol **13**: 459–465

Tsuda K, Somssich IE (2015) Transcriptional networks in plant immunity. New Phytol **206**: 932–947

Wang C, Shen L, Fu Y, Yan C, Wang K (2015) A simple CRISPR/Cas9 system for multiplex genome editing in rice. J Genet Genome **42**: 703–706

Wang Y, Wen T, Huang Y, Guan Y, Hu J (2018) Salicylic acid biosynthesis inhibitors increase chilling injury to maize (*Zea mays* L.) seedlings. Plant Growth Regul **86**: 11–21

Wu J, Kim SG, Kang KY, Kim JG, Park SR, Gupta R, Kim YH, Wang Y, Kim ST (2016) Overexpression of a pathogenesis-related protein 10 enhances biotic and abiotic stress tolerance in rice. Plant Pathol J **32**: 552–562

Yang C, Yu Y, Huang J, Meng F, Pang J, Zhao Q, Islam MA, Xu N, Tian Y, Liu J (2019) Binding of the *Magnaporthe oryzae* chitinase MoChia1 by a rice tetratricopeptide repeat protein allows free chitin to trigger immune responses. Plant Cell **31**: 172–188

Yang DL, Yang Y, He Z (2013) Roles of plant hormones and their interplay in rice immunity. Mol Plant **6**: 675–685

Zhang S, Zhu D, Li H, Zhang H, Feng C, Zhang W (2017) Analyses of mRNA profiling through RNA sequencing on a SAMP8 mouse model in response to ginsenoside Rg1 and Rb1 treatment. Front Pharmacol **8**: 88

Zhang Y, Tessaro MJ, Lassner M, Li X (2003) Knockout analysis of Arabidopsis transcription factors TGA2, TGA5, and TGA6 reveals their redundant and essential roles in systemic acquired resistance. Plant Cell **15**: 2647–2653